



1 **Analogue experiments on releasing and restraining bends and their application to**  
2 **the study of the Barents Shear Margin**

3  
4  
5  
6 **Roy H. Gabrielsen<sup>1)</sup>, Panagiotis A. Giannenas<sup>2)</sup>, Dimitrios Sokoutis<sup>1,3)</sup>, Ernst**  
7 **Willingshofer<sup>3)</sup>, Muhammad Hassaan<sup>1,4)</sup> & Jan Inge Faleide<sup>1)</sup>**

- 8  
9 <sup>1)</sup> Department of Geosciences, University of Oslo, Norway  
10 <sup>2)</sup> Univ Rennes, CNRS, Geosciences Rennes, UMR 6118, 35000, Rennes France  
11 <sup>3)</sup> Faculty of Geosciences, Utrecht University, the Netherlands  
12 <sup>4)</sup> Vår Energi AS, Grundingen 3, 0250 Oslo, Norway

13  
14  
15 **Corresponding author: Roy H. Gabrielsen ([r.h.gabrielsen@geo.uio.no](mailto:r.h.gabrielsen@geo.uio.no))**

16  
17 **ORCID iD:**  
18 Jan Inge Faleide: 0000-0001-8032-2015  
19 Roy H. Gabrielsen: 0000-0001-5427-8404  
20 Muhammad Hassaan: 0000-0001-6004-8557

21  
22  
23  
24  
25  
26  
27  
28  
29  
30  
31  
32  
33  
34  
35  
36  
37  
38  
39  
40  
41  
42  
43  
44  
45  
46  
47  
48  
49  
50  
51  
52  
53  
54  
55  
56



57 **Abstract:**  
58 The Barents Shear Margin separates the Svalbard and Barents Sea from the North  
59 Atlantic. It includes one northern (Hornsund Fault Zone) and a southern (Senja Fracture  
60 Zone) margin segment in which structuring was dominated by dextral shear. These  
61 segments are separated by the Vestbakken Volcanic Province that rests in a releasing  
62 bend position between the two. During the break-up of the North Atlantic the plate  
63 tectonic configuration was characterized by sequential dextral shear, extension,  
64 contraction and inversion. This generated a complex zone of deformation that contain  
65 several structural families of over-lapping and reactivated structures Although the  
66 convolute structural pattern associated with the Barents Shear Margin has been noted,  
67 it has not yet been explained in this framework.  
68 A series of crustal-scale analogue experiments, utilizing a scaled stratified sand-silicon  
69 polymer sequence, serve to study the structural evolution of the shear margin in  
70 response to shear deformation along a pre-defined boundary representing the geometry  
71 of the Barents Shear Margin and variations in kinematic boundary conditions of  
72 subsequent deformation events, i.e. direction of extension and inversion.  
73 The observations that are of particular significance for interpreting the structural  
74 configuration of the Barents Shear Margin are:  
75 1)The experiments reproduced the geometry and positions of the major basins and  
76 relations between structural elements (fault and fold systems) as observed along and  
77 adjacent to the Barents Shear Margin. This supports the present structural model for the  
78 shear margin.  
79 2) Several of the structural features that were initiated during the early (dextral shear)  
80 stage became overprinted and obliterated in the subsequent stages.  
81 3) Prominent early-stage positive structural elements (e.g. folds, push-ups) interacted  
82 with younger (e.g. inversion) structures and contributed to a complex final structural  
83 pattern.  
84 4) All master faults, pull-part basins and extensional shear duplexes initiated during the  
85 shear stage quickly became linked in the extension stage, generating a connected basin  
86 system along the entire shear margin at the stage of maximum extension.  
87 5) The fold pattern generated during the terminal stage (contraction/inversion) became  
88 dominant in the basinal areas and was characterized by fold axes with traces striking  
89 parallel to the basin margins. These folds, however, most strongly affected the shallow  
90 intra-basinal layers.  
91 This is in general agreement with observations in previous and new reflection seismic  
92 data from the Barents Shear Margin.  
93  
94  
95  
96  
97  
98  
99  
100  
101  
102  
103  
104  
105  
106



107 **Plain language summary:**

108 The Barents Shear Margin defines the border between the relatively shallow Barents  
109 Sea that is situated on a continental plate, and the deep ocean. This margin evolution  
110 history was probably influenced by the plate tectonic reorganizations. From scaled  
111 experiments we deduced several types of structures (faults, folds and sedimentary  
112 basins) that helps us to improve the understanding of the history of the opening of the  
113 North Atlantic.

114

115 **Key words:** Analogue experiments, dextral strike-slip, releasing and restraining bends,  
116 multiple folding, Barents Shear Margin, basin inversion

117

118

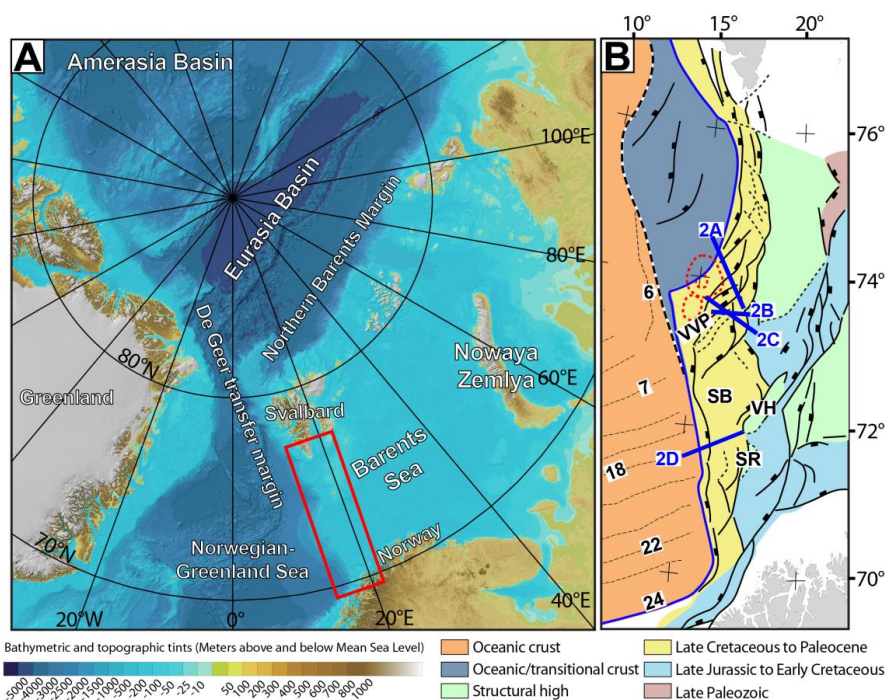


119 **Introduction**

120  
121 Physiography, width and structural style of the Norwegian continental margin vary  
122 considerably along its strike (e.g. Faleide et al. 2008, 2015). The margin includes a  
123 southern rifted segment between 60° and 70°N and a northern sheared-rifted segment  
124 between 70° and 82°N (**Figure 1A**). The latter coincides with the ocean-ward border of  
125 the western Barents Sea and Svalbard margins (e.g. Faleide et al. 2008) and is referred  
126 to here as “the Barents Shear Margin”. This segment coincides with the continent-ocean  
127 transition (COT) of the northernmost part of the North Atlantic Ocean, and its  
128 configuration is typical for that of transform margins where the structural pattern  
129 became established in an early stage of shear, later to develop into an active continent-  
130 ocean passive margin (Masclé & Blarez 1987; Lorenzo 1997; Seiler et al. 2010; Basile  
131 2015; Nemcok et al. 2016).

132 Late Cretaceous - Palaeocene shear, rifting, breakup and incipient spreading in the  
133 North Atlantic was associated with voluminous magmatic activity, resulting in the  
134 development of the North Atlantic Volcanic Province (Saunders et al. 1997; Ganerød  
135 et al. 2010; Horni 2017). According to its tectonic development, the Barents Shear  
136 Margin (**Figure 1B**) incorporates, or is bordered by, several distinct structural elements,  
137 some of which are associated with volcanism and halokinesis.

138 The multistage development combined with a complex geometry caused interference  
139 between structures (and sediment systems) in different stages of the margin  
140 development. Such relations are not always obvious, but interpretation can be supported  
141 by the help of scale-models. In combining the interpretation of reflection seismic data  
142 and analogue modeling, therefore, we investigate structures generated in (initial)  
143 dextral shear, the development into seafloor spreading and subsequent contraction in  
144 this process, the later stages of which were likely influenced by plate reorganization  
145 (Talwani & Eldholm 1977, Gaina et al. 2009, see also see also Vågnes et al. 1998;  
146 Pascal & Gabrielsen 2001; Pascal et al. 2005; Gac et al. 2016) or other far-field stresses  
147 (Doré & Lundin 1996; Lundin & Doré 1997; Doré et al. 1999; 2016; Lundin et al.  
148 2013). The present experiments were designed to illuminate the structural complexity  
149 affiliated with multistage sheared passive margins, so that the significance of structural  
150 elements like fault and fold systems observed along the Barents Shear Margin could be  
151 set into a dynamic context.



152  
153 Figure 1: A) The Barents Sea provides is separated from the Norwegian-Greenland Sea  
154 by the de Geer transfer margin. Red box shows the present study area. B) Structural  
155 map Barents Sea shear margin. Note segmentation of the continent-ocean transition.  
156 Abbreviations: HFZ=Hornsund Fault Zone, KFC = Knølegga Fault Complex,  
157 SFZ=Senja Shear Zone, SR=Senja Ridge, SB = Sørvestsnaget Basin, VVP =  
158 Vestbakken Volcanic Province.  
159

### 160 Regional background

161 In the following sections we provide definitions and a short description of the most  
162 important structural elements constituting the study area. All structural elements  
163 described below are displayed in **Figure 1B**.

164

165 **The Barents Shear Margin** was preceded by the “De Geer Zone” (Eldholm et al. 1987;  
166 2002; Faleide et al. 1988; Breivik et al. 1998; 2003). Together with its conjugate  
167 Greenland counterpart it carries the evidence of an extensive period of structuring,  
168 starting with post-Caledonian (Devonian) extension and culminating with Cenozoic  
169 break-up of the North Atlantic (e.g. Brekke 2000; Gabrielsen et al. 1990; Faleide et al.  
170 1993; Gudlaugsson et al. 1998). Two shear margin segments that are separated by a  
171 central rift-dominated segment can be identified in the Barents Shear Margin (Myhre  
172 et al. 1982; Vågnes 1997; Myhre & Eldholm 1988; Ryseth et al. 2003; Faleide et al.



173 1988; 1993; 2008). Each segment maintained a particular signature concerning the  
174 structural and magmatic characteristics of the crust during its development. Of these  
175 the Senja Shear Margin is the southernmost segment, originally termed the Senja  
176 Fracture Zone by Eldholm et al. (1987). Particularly the hanging wall west of the  
177 Knølegga Fault Complex of the Barents Shear Margin was affected by wrench  
178 deformation as seen from several push-ups and fold systems (Grogan et al. 1999; Bergh  
179 & Grogan 2003). Here, NNW-SSE-striking folds interfere with folds with NE-SW-  
180 striking axes (Giennenas 2018). Strain partitioning may also have affected some of the  
181 other shear zone segments of the study area (Kristensen et al. 2017).

182

183 **The Senja Shear Margin** was active during the Eocene opening of the Norwegian-  
184 Greenland Sea during dextral shear that was accompanied splitting out slivers of  
185 continental crust that became isolate units embedded by oceanic crust during seafloor  
186 spreading (Faleide et al 2008). The Senja Shear Margin coincides with the western  
187 margin of a basin system that is characterized by significant crustal thinning and  
188 extreme sedimentary thicknesses that may approach 18-20km. This part of the shear  
189 margin was characterized by a composite architecture even at the earliest stages of its  
190 development (Faleide et al. 2008). Subsequently shearing contributed to the  
191 development of releasing and restraining bends, associated pull-apart-basins, neutral  
192 strike-slip segments, flower-structures and fold-systems (*sensu* Crowell 1974a,b;  
193 Biddle & Christie-Blick 1985a,b; Cunningham & Mann 2007a,b). The structuring of  
194 the margin was complicated by active halokinesis (Knutsen & Larsen 1997;  
195 Gudlaugsson et al. 1998; Ryseth et al. 2003).

196

197 **The Hornsund Fault Zone and West Spitsbergen Fold-and Thrust Belt** form the  
198 northernmost segment of the Barents Shear Margin and coincides with the northern  
199 continuation of the De Geer Zone and the Senja Shear Margin. The presently  
200 distinguishable master fault of this system is the Hornsund Fault Zone, which together  
201 with the West Spitsbergen fold-and-thrust-belt provides a classical setting for  
202 transpression and strain partitioning (Harland 1965; 1969; 1971; Lowell 1972;  
203 Gabrielsen et al. 1992; Maher et al. 1997; Leever et al. 2011 a,b). Plate tectonic  
204 reconstructions suggest that the plate boundary accommodated c. 750 km along-strike  
205 displacement and 20-40 km of shortening in the Eocene (Bergh et al. 1997; Gaina et al.  
206 2009).



207

208 **The Sørvestsnaget Basin** occupies the area east the COT between 71 and 73°N and is  
209 characterized by an exceptionally thick Cretaceous-Cenozoic sequence (Gabrielsen et  
210 al. 1990). To the west it is delineated by the Senja Shear Margin and to the northeast it  
211 is separated from the Bjørnøya Basin by the southern part of the Knølegga Fault  
212 Complex (Faleide et al. 1988). The Senja Ridge coincides with its southeastern border,  
213 whereas the Vestbakken Volcanic Province is situated to its north. An episode of  
214 Cretaceous rifting in the Sørvestsnaget Basin seems to have climaxed in the  
215 Cenomanian-middle Turonian (Breivik et al. 1998) to become succeeded by Late  
216 Cretaceous-Palaeocene fast sedimentation (Ryseth et al. 2003). Particularly the later  
217 stages of the basin development were likely strongly influenced by the opening of the  
218 North Atlantic (Hanisch 1984; Brekke & Riis 1987). Salt diapirism did also contribute  
219 to structuring of this basin (Perez-Garcia et al. 2013).

220

221 **The Senja Ridge** runs parallel to the continental margin and coincides with the western  
222 border of the Tromsø Basin. It is characterized by a N-S-trending gravity anomaly  
223 which are interpreted as buried mafic-ultramafic intrusions which are associated with  
224 the Seiland Igneous Province (Fichler & Pastore 2022). The structural development of  
225 the Senja Ridge has been linked to shear affiliated with the development of the shear  
226 margin (Riis et al. 1986).

227

228 **The Knølegga Fault Complex** can be seen as a part of the Hornsund fault system  
229 extending from the southern tip of Spitsbergen (Gabrielsen et al. 1990). It trends NNE-  
230 SSW to N-S and defines the western margin of the Stappen High. The vertical  
231 displacement approaches 6 km. Although the main movements along the fault may be  
232 Tertiary of age, it is likely that it was initiated much earlier. The Tertiary displacement  
233 may have had a lateral (dextral) component (Gabrielsen et al. 1990).

234

235 **The Vestbakken Volcanic Province** is the central topic of the present contribution. It  
236 represents the rifted segment of the Senja Shear Margin and links the sheared margin  
237 segments that are situated to the north and south of it and occupies a typical right-double  
238 stepping (eastward) releasing-bend-setting. Prominent volcanoes and sill-intrusions  
239 display significant magmatic activity, and three distinct volcanic events are  
240 distinguished in the Vestbakken Volcanic Province (Jebsen & Faleide 1998; Faleide et



241 al. 2008; Libak et al. 2012). The area has been affected by complex tectonics and both  
242 extensional and contractional structures are observed. The Vestbakken Volcanic  
243 Province is delineated towards the east by an extensional top-west fault zone that  
244 parallels the Knølegga Fault Complex). The interior of the Vestbakken Volcanic  
245 Province is dominated by NE-SW-striking extensional faults and associated fault  
246 blocks. Positive structural elements include inverted fault blocks, and wide-angle ( $\lambda >$   
247 20 km) anticlines (roll-over anticlines?) and domes that are overprinted by faults and  
248 folds with amplitudes and wavelengths on the hundred- and km-scales.

249 The eastern boundary fault (EBF) is a top-west normal fault with a regional NNE-SSW  
250 strike, consisting of two separate, hard-linked segments. Its northern segment dips  
251 more steeply to the WNW than the southern segment. The total vertical displacement  
252 as measured on the early Eocene level is in the order of 300 msec (450m), and the upper  
253 part of the hanging wall displays a normal drag modified by hanging wall tight anticline  
254 suggesting post early Miocene inversion. Several normal, dominantly NE-SW-striking  
255 NW-facing normal faults transect the hanging wall of the EFB-fault. The Central Fault  
256 (CF) is the largest of those and is hard-linked to the central segment of the EFB-fault is  
257 the largest of those. The Central Fault is the most prominent fault of a NW-SE-striking  
258 fault population that characterizes the entire Vestbakken Volcanic Province. Three  
259 episodes of Cenozoic extensional faulting were identified in the Vestbakken Volcanic  
260 Province: (i) a late Paleocene-early Eocene event, which correlates in time with the  
261 continental break-up in the Norwegian-Greenland Sea, (ii) an early Oligocene event is  
262 tentatively correlated to plate reorganization around 34 Ma activated mainly NE-SW  
263 striking faults and (iii) an extensional Pliocene event. Evidence of volcanic activity  
264 coincide with the first two of these events. The Vestbakken Volcanic Province is  
265 constrained to its east by the eastern boundary fault (EBF in **Figure 1B**), that is a part  
266 of the Knølegga Fault Complex, separating the Vestbakken Volcanic Province from the  
267 marginal Stappen High further to the east. To the south and southeast the Vestbakken  
268 Volcanic Province drops gradually into the Sørvestsnaget Basin across the southern  
269 extension of the eastern boundary fault and its associated faults. To the west and north  
270 the area is delineated by the continent – ocean boundary/transition (marked as COB in  
271 Fig. 4.1). The Vestbakken Volcanic Province includes both extensional and  
272 contractional structures (e.g. Jebesen & Faleide, 1998; Faleide et al., 2008; Blaich et al.,  
273 2017). Cenozoic tectonic activity has left its imprint at the eastern part of the study area.  
274 All other faults in this map are secondary faults, mainly acting as accommodation



275 structures to the master faults. Starting from the southern part of the area and south of  
276 the well site, a population of secondary faults is expressed as anastomosing faults  
277 traces.

278

### 279 **Reflection seismic data**

280 The data set of this study includes 2D seismic reflection data from several surveys and  
281 well data in the Vestbakken Volcanic Province. Data coverage is less dense in northern  
282 part of the study area. Typical spacing of seismic lines is 4km. Well 7316/5-1 was used  
283 to correlate the seismic data with formation tops in the study area whereas published  
284 paper based correlations provided calibration and age of each seismic horizon mapped  
285 (e.g. Eidvin et al., 1993; 1998 Ryseth et al., 2003). Three stratigraphic groups are  
286 present in the well; the Nordland Group (473 - 945 m); the Sotbakken Group (945-  
287 3752m) and Nygrunnen Group (3752-4014m) (Eidvin et al., 1993; 1998;  
288 [www.npd.com](http://www.npd.com)).

289

### 290 **Fold families**

291 Several folds of regional significance (with axial traces that can be followed along  
292 strike for 2-3 km or more) occur in the Vestbakken Volcanic Province. The folds  
293 commonly are situated in the hanging walls of extensional fault, some of which bear  
294 the characteristics of tectonic inversion. The fold axial traces parallel the fault traces or  
295 are situated in the strike-continuation of such. It therefore seems obvious that the  
296 structural grain, as defined by the thick-skinned master faults strongly influenced the  
297 positions of the subsequent folds. The continuity of these structures remains obscure  
298 due to spacing of reflection seismic lines, so each fold may include undetected overlap  
299 zones or axial off-sets that have not been detected. The folds were identified on the  
300 lower Eocene, Oligocene and lower Miocene levels. All the mapped folds are either  
301 positioned in the hanging walls of extensional (sometimes inverted) master faults or are  
302 dissected by younger faults with minor throws.

303

304 Three basic fold families were identified in the Vestbakken Volcanic Province by  
305 Giennenas (2018): *Fold family 1* (**Figure 2**) consists of gentle to open anticline-syncline  
306 pairs with upright to slightly inclined axial planes, sometimes with shallowly plunging  
307 fold axes and saddle points, so that the folds are not strictly cylindrical. Folds of this

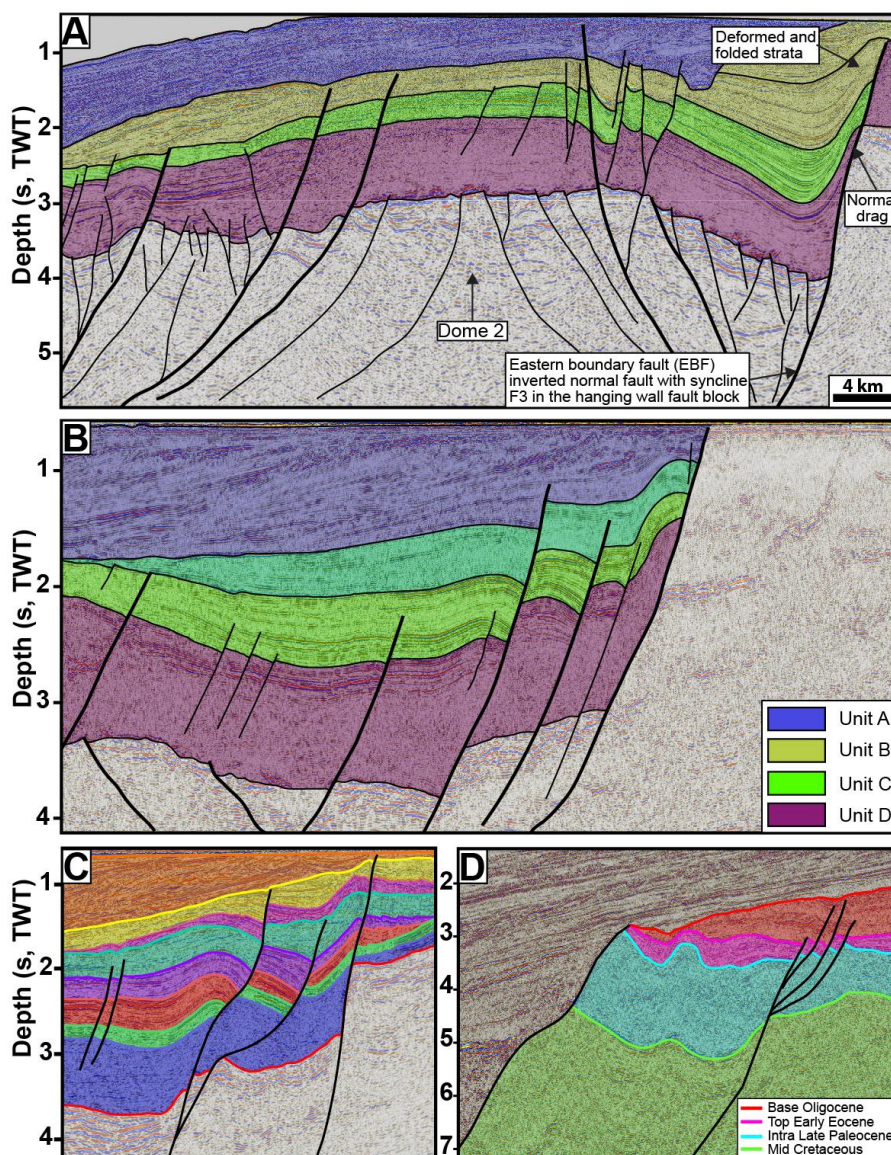


308 family strikes dominantly NE-SW to NNE-SSW and are generally situated at some  
309 distance from the master basin margin faults and in the central parts of the Vestbakken  
310 Volcanic Province where larger faults are less abundant. The wavelengths are in the  
311 order of 3-10 km and the amplitudes may reach 400 m. The fold flanks sometimes  
312 display smaller open folds with wavelengths on the hundred-meter-scale that may be  
313 parasitic, whereas the central parts are commonly broken by post-folding steep brittle  
314 normal faults that define separate fault zones that are separate from the major folds  
315 along strike (see Fold family 3 below). *Fold family 2* includes folds with inclined axial  
316 planes with dominantly long NW-limbs and short SE-limbs (**Figure 2**), which are more  
317 common along the basin margin and in affiliation with low-angle intra-basin reverse  
318 faults. These generally have the characteristics of fault-propagation folds and are  
319 positioned in the hanging walls with steep, inverted normal faults. These are  
320 characterized of axial planes with dips of up to 45 deg) and snake-head-geometries  
321 commonly found in the hanging walls of master faults (**Figure 2A, B**). Fold family  
322 includes anticline-syncline pairs with fold axes that are parallel and are situated more  
323 distally to the eastern boundary fault (EBF) and are found internally in extensional fault  
324 blocks. The fold axes of the latter sub-family have up-right axial planes and are  
325 accordingly generally oriented N-S

326

### 327 **Strike-slip systems and analogue shear experiments**

328 Shear margins and strike-slip systems are structurally complex and highly dynamic,  
329 meaning that the incipient and mature stages of strike-slip deformation commonly  
330 display a variety of geometries (e.g. Graymer et al. 2007) making it hard to comprehend  
331 the full complexity solely through fieldwork (e.g. Crowell 1962, 1974a,b; Woodcock  
332 & Fischer 1986; Mousloupoulou et al. 2007; 2008). Analogue



333

334 Figure 2: Seismic examples, Vestbakken Volcanic Province. A) Gentle, partly  
335 collapsed NE-SW-striking anticline/dome of fold family 1 (Giannenas 2018) of  
336 uncertain origin in the eastern terrace domain of the southern Vestbakken Volcanic  
337 Province. This may be a remnant, rotated PSE-1-structure (see text for explanation).  
338 B,C) Assymetrical folds (fold family 2; Giannenas 2018) situated along the eastern  
339 margin of the Vestbakken Volcanic Province. These may represent primary SPE-5-  
340 structures focused in the hangingwalls along margins of master fault blocks, or  
341 reactivated SPE-2-structures. D) trains of symmetrical folds with upright fold axes  
342 (corresponding to PSE-5-structures are preserved inside larger fault blocks. See text  
343 for explanation of SPE-structures.



344 models illustrate such complexity well and therefore attracted the attention of early  
345 workers in this field (e.g. Cloos 1928; Riedel 1929) and have continued to do so until  
346 today. Early experimental works mostly utilized one-layer (“Riedel-box”) models (e.g.  
347 Emmons 1969; Tchalenko 1970; Wilcox et al. 1973), which were soon to be expanded  
348 by the study of multilayer systems (e.g. Faugère et al. 1986; Naylor et al. 1986; Richard  
349 et al. 1991; Richard & Cobbold 1989, 1995; Schreurs 1994, 2003; Manduit & Dauteuil  
350 1996; Dauteuil & Mart 1998; Schreurs & Colletta 1998, 2003; Ueta et al. 2000; Dooley  
351 & Schreurs 2012). The systematics and dynamics of strike-slip systems have been  
352 focused upon in a number of summaries like Sylvester (1985, 1988); Biddle & Christie-  
353 Blick (1985a,b); Cunningham & Mann (2007); Dooley & Schreurs (2012); Nemcok et  
354 al. (2016) and Peacock et al. (2016). Concepts and nomenclature established in these  
355 works are used in the following descriptions and analysis. Also, following Christie-  
356 Blick & Biddle (1985a,b) and Dooley & Schreurs (2012) we apply the term Principal  
357 Deformation Zone (PDZ) for the junction between the movable polythene plates  
358 underlying the experiment. The contact between the fixed and movable base defined a  
359 non-stationary velocity discontinuity (“VD”; Ballard et al. 1987; Allemand & Brun  
360 1991; Tron & Brun 1991).

361 Several experimental works have particularly focused on the geometry and  
362 development of pull-apart-basins in releasing bend settings (Mann et al. 1983; Faugère  
363 et al. 1983; Richard et al. 1995; Dooley & McClay 1997; Basile & Brun 1999; Sims et  
364 al. 1999; Le Calvez & Vendeville 2002; Mann 2007; Mitra & Paul 2011). The pull-  
365 apart basin was described by Burchfiel & Stewart (1966) and Crowell (1974a,b) as  
366 formed at a releasing bend or at a releasing fault step-over along a strike-slip zone  
367 (Biddle & Christie-Blick 1985a,b). This basin type has also been termed “rhomb  
368 grabens” (Freund 1971) and “strike-slip basins” (Mann et al. 1993) and is commonly  
369 considered to be synonymous with the extensional strike-slip duplex (Woodcock &  
370 Fischer 1986; Dooley & Schreurs 2012). In the descriptions of our experiments, we  
371 found it convenient to distinguish between extensional strike-slip duplexes in the  
372 context of Woodcock & Fischer (1986) and Twiss & Moores 2007, p. 140-141;) and  
373 pull-apart basins (rhomb grabens: Crowell 1974a,b; Aydin & Nur 1993) since they  
374 reflect slightly different stages in the development in our experiments (see discussion).

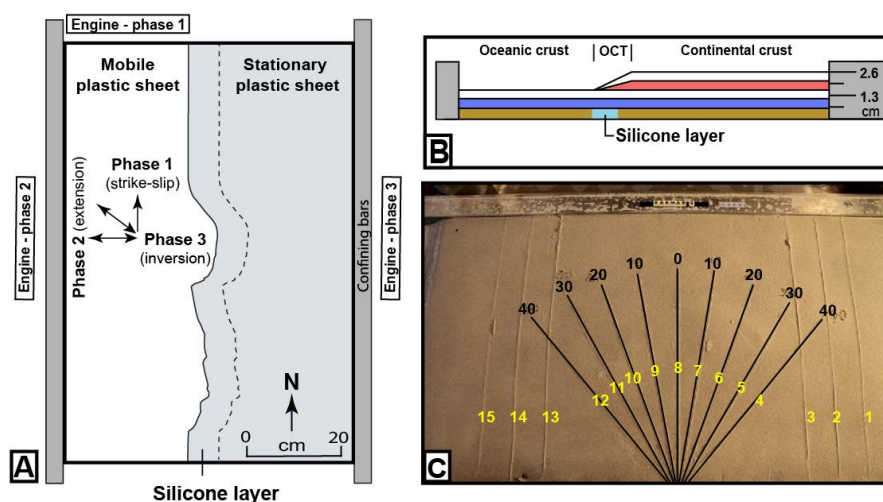
375

376



## 377 **Experimental setup**

378 To study the kinematics of complex shear margins, a series of analogue experiments  
379 were performed at the tectonic modelling laboratory (TecLab) of Utrecht University,  
380 The Netherlands. All experiments were built on two overlapping 1 mm thick plastic  
381 sheets (each 100 cm long and 50 cm wide) that were placed on a flat, horizontal table  
382 surface. The boundary between the underlying movable and overlaying stationary  
383 plastic sheets had the shape of the mapped continent-ocean boundary (COB; **Figure**  
384 **1B**). The moveable sheet was connected to an electronic engine, which pulled the sheet  
385 at constant velocity. The modelling material was then placed on these sheets where the  
386 layers on the stationary sheet represent the continental crust including the continent-  
387 ocean transition (COT) whereas the those on the mobile sheet represents the oceanic  
388 crust. The model layers are confined by aluminum bars along the long sides and sand  
389 along the short sides (**Figure 3A**). Continental crust tapers off towards the oceanic crust  
390 simulating the ocean-continent transition (**Figure 3B**) were included in all models.  
391

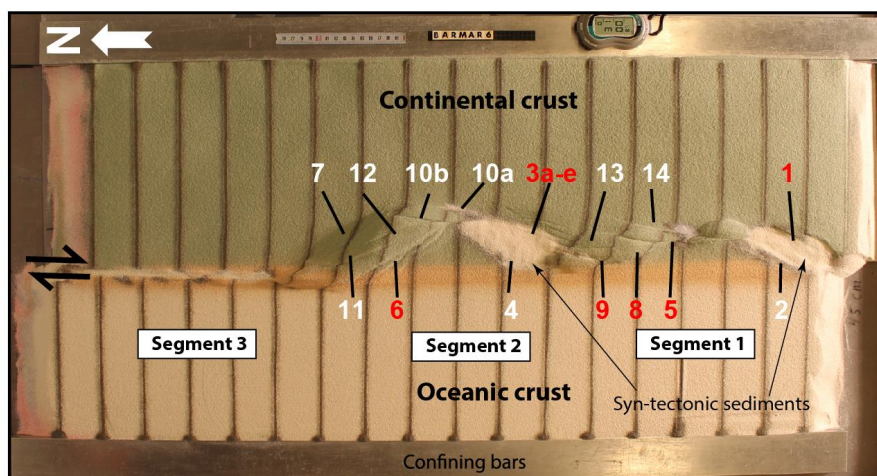


392  
393 Figure 3: A) Schematic set-up of BarMar3-experiment as seen in map view. B)  
394 Section through same experiment before deformation, indicating stratification  
395 and thickness relations. C) Standard positions and orientation for sections cut in all  
396 experiments in the BarMar-series. Yellow numbers are section numbers. Black  
397 numbers indicate angle between the margins of the experiment (relative to N-S) for  
398 each profile.  
399

400  
401



402  
403 The pre-cut shape of the plate boundary includes major releasing bends positioned so  
404 that they correspond to the geometry of the COB and the three main structural segments  
405 of the Barents Shear Margin as follows. *Segment 1* of the BarMar-experiments (**Figure**  
406 **4**) contained several sub-segments with releasing and restraining bends as well as  
407 segments of “neutral” (Wilcox et al. 1973; Mann et al. 1983; Biddle & Christie-Blick  
408 1985b) or “pure” (Richard et al. 1991) strike-slip. *Segment 2* had a basic crescent shape,  
409 thereby defining a releasing bend at its southern margin in the position similar to that  
410 of the Vestbakken Volcanic Province, that merged into a neutral shear-segment along  
411 the strike of, whereas a restraining bend occupied the northern margin of the segment.  
412 *Segment 3* was a straight basement segment, defining a zone of neutral shear and  
413 corresponds to the strike-slip segment west of Svalbard (**Figure 1**).  
414



415  
416 Figure 4: Position of segments and major structural elements as referred to in the text  
417 and subsequent figures (see particularly Figures 5 and 6). This example is taken from  
418 the reference experiment BarMar6. All experiments BarMar6-9 followed the same  
419 pattern, and the same nomenclature was used in the description of these experiments.  
420  
421 The experiments included three stages of deformation with constant rates of movement  
422 of the mobile sheet at  $10 \text{ cm hr}^{-1}$  in all three stages. Dextral shear was applied in the *first*  
423 *phase* in all experiments by pulling the lower plastic sheet by 5cm. In the *second phase*  
424 the left side of the experiment was extended by 3 cm orthogonally (BarMar6) or  
425 obliquely (325 degrees; BarMar 8 & 9) to the trend of the shear margin, whereas plate  
426 motion was reversed during the *third phase of deformation*, leading to inversion of



427 earlier formed basins that had been developed in the strike-slip and extensional phases.  
428 Sedimentary basins that develop due to strike-slip (phase 1) or extension (phase 2) have  
429 been filled with layers of colored feldspar sand by sieving. These layers are primarily  
430 important for discriminating among deformation phases and thus act as marker  
431 horizons. Phase 3 was initiated by inverting the orthogonal (BarMar6) or oblique  
432 (BarMar 8 & 9,) extension of Phase 2 as a proxy for ridge-push that likely was initiated  
433 when the mid-oceanic ridge was established in Miocene time in the North Atlantic  
434 (Moser et al., 2002; Gaina et al. 2009). Contraction generated by ridge-push has been  
435 inferred from the mid Norwegian continental shelf (Våagnes et al. 1998; Pascal &  
436 Gabrielsen 2001; Faleide et al. 2008; Gac et al. 2016) and seems still to prevail in the  
437 northern areas of Scandinavia (Pascal et al., 2005), although far-field compression  
438 generated by other processes have been suggested (e.g. Doré & Lundin 1996).  
439 Coloured layers of dry feldspar sand represent the brittle oceanic and continental crust.  
440 This material has proven suitable for simulating brittle deformation conditions  
441 (Willingshofer et al., 2005; Luth et al. 2010; Auzemery et al., 2021) and is characterized  
442 by a grain size of 100-200  $\mu\text{m}$ , a density of 1300  $\text{kgm}^{-3}$ , a cohesion of  $\sim 16\text{-}45$  Pa and a  
443 peak friction coefficient of 0.67 (Willingshofer et al. 2018). Additionally, a 8 mm thick  
444 and of variable width corresponding to the mapped transition zone of 'Rhodorsil  
445 Gomme GSIR' (Sokoutis, 1987) silicone putty mixed with fillers was used as a proxy  
446 for the thinned and weakened continental crust at the ocean-continent transition (**Figure**  
447 **1B and 3A,B**). This Newtonian material ( $n=1.09$ ) has a density of 1330  $\text{kgm}^{-3}$  and a  
448 viscosity of  $1.42 \times 10^4$  Pa.s.  
449 The experiments have been scaled following standard scaling procedures as described  
450 by Hubbert (1937), Ramberg (1967) or Weijermars and Schmeling (1986), assuming  
451 that inertia forces are negligible when modelling tectonic processes on geologic  
452 timescales (see Ramberg (1981) and Del Ventisette et al., (2007) for a discussion on  
453 this topic). The models were scaled so that 10 mm in the model approximates c. 10 km  
454 in nature yielding a length scale ratio of  $1.00 \times 10^{-6}$ . As such, the model oceanic and  
455 continental crusts scale to 18 and 26 km in nature, respectively, which, although slightly  
456 overestimating the most intensely thinned oceanic crust (10-12 km) is in full agreement  
457 with the estimated thickness of the thinned oceanward segment of the continental crust  
458 (30-20 km Breivik et al. 1998).  
459 The brittle crust, dry feldspar sand, deforms according to the Mohr-Coulomb fracture  
460 criterion (Horsfield 1977; Mandl et al. 1977; McClay 1990; Richard et al. 1991;



461 Klinkmüller et al. 2016), whereas silicone putty promotes ductile deformation and  
462 folding. The geometry applied in the present experiments is accordingly well suited for  
463 the study of the COB in the Barents Shear Margin (Breivik et al. 1998).

464 When complete, the experiments were covered with a thin layer of sand further to  
465 stabilize the surface topography before the models were saturated with water and cross-  
466 sections that were oriented transverse to the velocity discontinuity were cut in a fan-  
467 shaped pattern (**Figure 3C**). All experiments have been monitored with a digital camera  
468 providing top-view images at regular time intervals of one minute.

469

470 All experiments performed were oriented in a N-S-coordinate framework to facilitate  
471 comparison with the western Barents Sea area and had a three-stage deformation  
472 sequence (dextral shear – opening – closure). All descriptions and figures relate to this  
473 orientation. It was noted that all experiments reproduced comparable basic geometries  
474 and structural types, demonstrating robustness against variations in contrasting strength  
475 of the “ocean-continent”-transition zone, which included by a zone of silicone putty  
476 with variable width below a eastward thickening sand-wedge (**Figure 3B**) and changing  
477 displacement velocities.

478

### 479 **Modelling Results**

480 A series of totally nine experiments (BarMar1-9) with the set-up described above was  
481 performed. Experiments BarMar1-5 were used to calibrate and optimize geometrical  
482 outline, deformation rate, and angles of relative plate movements and are not shown  
483 here. The optimized geometries and experimental conditions were utilized for  
484 experiments BarMar6-9, of which BarMar6 and 8 (and some examples from BarMar9  
485 and are illustrated here, yielded similar results in that all crucial structural elements  
486 (faults and folds) were reproduced in all experiments as described in the text are shown  
487 in **Figure 4**.) It is emphasized that the extensional basins affiliated with the extension  
488 phase (phase 2) became wider in the orthogonal (BarMar6) as compared to oblique  
489 extension experiments (BarMar 8) (**Figures 5 and 6**). Furthermore, the fold systems  
490 generated in the experiments that utilized oblique contraction of  $325/145^0$  (BarMar8-9)  
491 produced more extensive systems of non-cylindrical folds with continuous, but more  
492 curved fold traces as compared experiments with orthogonal extension/contraction  
493 (BarMar6). The fold axes generally rotated to become parallel to the (extensional)



494 master faults delineating the pull-apart basins generated in deformation stage 1 in  
495 experiments with an oblique opening/closing angle.

496 Examples of the sequential development is displayed in **Figures 5 and 6**) and  
497 summarized in **Figure 7**.

498 Elongate positive structural elements with fold-like morphology as seen on the surface  
499 were detected during the various stages of the present experiments. The true nature of  
500 those were not easily determined until the experiments were terminated and transects  
501 could be examined. Such structures included buried push-ups (*sensu* Dooley &  
502 Schreurs 2012), antiformal stacks, back-thrusts, positive flower structures, fold trains,  
503 and simple anticlines. For convenience, we use the non-genetic term “positive structural  
504 elements” termed *PSEm-n* for such structure types as seen in the experiments in the  
505 following description.

506 In the following the deformation in each segment is characterized for the three  
507 deformation phases.

508

509

#### 510 **Deformation phase 1: Dextral shear stage**

511

512 *Segment 1*: Differences in the geometry of the pre-cut fault trace between segments 1,  
513 2 and 3 became evident after the very initial deformation stage. Particularly in segments  
514 1 and 3 an array of oblique *en échelon* folds in between Riedel shear structures (*PSE-*  
515 *1-structures*) oriented c. 145°(NW-SE) to the regional VD rotating into a NNW-SSE-  
516 orientation by continued shear (**Figure 8**; see also Wilcox et al. 1973; Ordonne &  
517 Vialon 1983; Richard et al. 1991; Dooley & Schreurs 2012). These were simple,  
518 harmonic folds with upright axial planes and fold axial traces extending a few cm  
519 beyond the surface shear-zone described above. They had amplitudes on the scale of a  
520 few millimeters and wavelengths on scale of 5 cm. The PSE-1-structures interfered with  
521 or were dismembered by younger developing structures, also causing northerly rotation  
522 of individual intra-fault zone lamellae (remnant PSE-1-structures (**Figure 8**). Structures  
523 similar to PSE-1-fold arrays are known from almost all strike-slip experiments reported  
524 and described in the literature from the early works of (e.g. Cloos 1928; Riedel 1929.  
525 See Dooley & Schreurs 2012 for summary) and are therefore not given further attention  
526 here. By 0.25 cm of horizontal displacement in segment 1, which included two releasing  
527 and restraining bends in combination with strands of neutral shear, a slightly curvilinear



528 surface trace of a NE-SW-striking, top-NW normal fault in the southernmost part of  
529 segment 1 developed. This co-existed with the PSE-1-structures and was immediately  
530 paralleled by a normal fault with opposite throw (fault 2, **Figure 4**) so that the two  
531 faults constrained a crescent- or spindle-shaped incipient extensional shear duplex  
532 (**Figures 5B and 6B**; see also Mann et al. 1983; Christie-Blick & Biddle 1985; Mann  
533 2007; Dooley & Schreurs 2012).

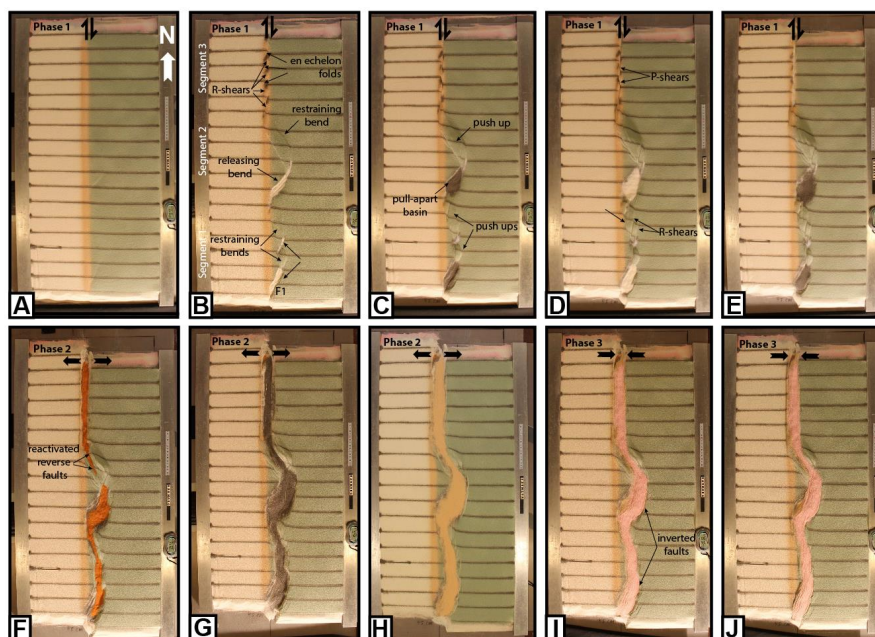
534 A system of *en échelon* separate N-S to NNE-SSE- striking normal and shear fault  
535 segments became visible in segment 1 after ca. 1 cm of shear (**Figure 5C,D**). These  
536 faults did not have the orientations as expected for R- and R'-shears, but became  
537 progressively linked by along-strike growth and the development of new faults and fault  
538 segments. They thereby acquired the characteristics of Y-shears, dissecting the PSE-1-  
539 structures). By 2.4 cm of shear, segment 1 had become one unified fault array (**Figure**  
540 **5D and 6D**), delineating a system of incipient push-ups or positive flower structures  
541 (*PSE-2-structures*; **Figures 8 and Figure 10, sections B1 and B3**, see also; Riedel  
542 1929; Wilcox et al. 1973; Odonne & Vialon 1983; Dauteuil & Mart 1995; Dooley &  
543 Schreurs 2012).

544 The PSE-2-structures had amplitudes of 1 - 2 cm and wavelengths of 3 - 5 cm as  
545 measured on the surface with fault surfaces that steeped down-section, the deepest parts  
546 of the structures having cores of sand-layers deformed by open to tight folds. The folds  
547 had upright or slightly inclined axial planes, dipping up to 55°, mainly to the east. The  
548 structures also affected the shallowest layers down to 1-2 cm in the sequence, but the  
549 shallowest sequences were developed at a later stage of deformation and were  
550 characterized by simple gentle to open anticlines.

551 These structures were constrained to a zone of deformation directly above the trace of  
552 the basement fault, similar to that commonly seen along shear zones (e.g. Tchalenko  
553 1971; Crowell 1974 a,b; Dooley & Schreurs 2012). This zone was 3-4 cm wide and  
554 remained stable throughout deformation stage 1 and was restricted to the close vicinity  
555 of the basement shear fault itself as also described from one-stage shear faults in Riedel  
556 box-type experiments (e.g. Tchalenko 1970; Naylor et al. 1986; Richard et al. 1991;  
557 Casas et al. 2001; Dauteuil & Mart 1998; Dooley & Schreurs 2012) and from nature as  
558 well (e.g. Wilcox et al. 1973; Harding 1974; Harding & Lowell 1979; Sylvester 1988;  
559 Woodcock & Schubert 1994; Mann 2007).

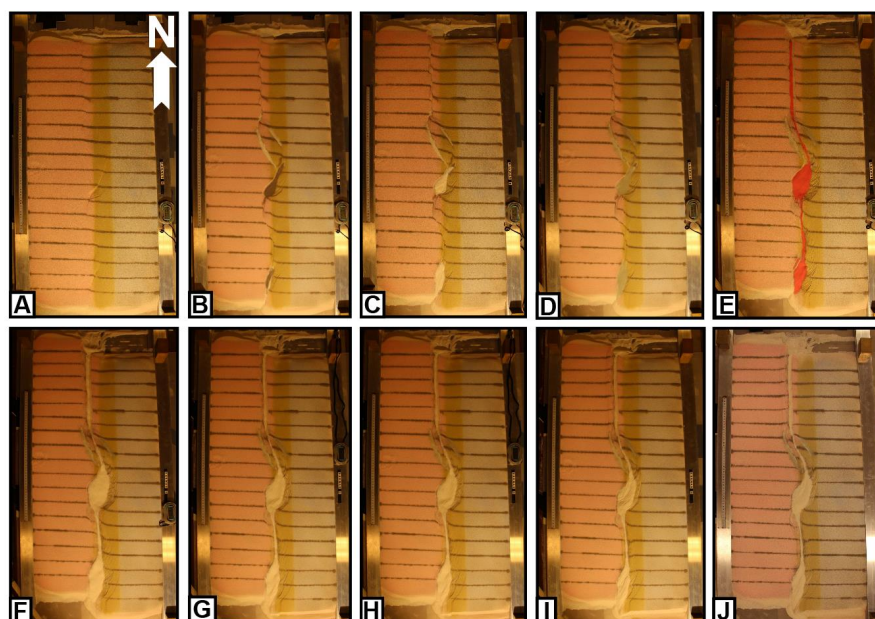


560 A horse-tail-like fault array developed by ca. 3 cm of shear at the transitions between  
561 segments 1 and 2 (see also Cunningham & Mann 2007; Dooley & Schreurs 2012, their  
562 Figure 44) (**Figures 5B-D and 6B-D**).  
563



564  
565 Figure 5: Sequential development of experiment BarMar6 by 0.5, 2.4, 3.5, 4.0 and  
566 5.0cm of dextral shear (Steps A-E), orthogonal extension (steps F-H) and oblique  
567 contraction (steps I-J). The master fault strands are numbered in Figure 4, and the  
568 sequential development for each structural family is shown in Figure 7.  
569

570 The structuring in *Segment 2*; was ruled by the crescent-shaped basement fault (VD)  
571 that generated a releasing bend along its southern and a restraining bend along its  
572 northern border (**Figure 11**). The first fault of fault array 3a-e in the southern part of  
573 *Segment 2* was activated after c. 0.15 cm of bulk horizontal displacement (**Figure 7**).  
574 It was situated directly above the southernmost pre-cut releasing bend, defining the  
575 margin of crescent-shaped incipient extensional strike-slip duplexes (in the context of  
576 Woodcock & Fischer, 1986, Woodcock & Schubert, 1994 and Twiss & Moores, 2007,  
577 p. 140-141). The developing basin got a spindle-shaped structure and developed into a  
578 basin with a lazy-S-shape (Cunningham & Mann 2007; Mann 2007).  
579

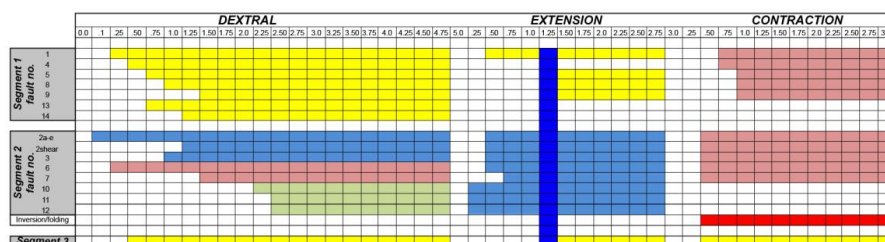


580

581 Figure 6: Sequential development of experiment BarMar8 by 0.5, 2.4, 3.5, 4.0 and  
582 5.0cm of dextral shear (Steps A-E), oblique extension (steps F-H) and oblique  
583 contraction (steps I-J). The master fault strands are numbered in Figure 3, and the  
584 sequential development for each structural family is shown in Figure 7. Phases 2 and 3  
585 involved oblique (3250) extension and contraction in this experiment.  
586

587 The basin widened towards the east by stepwise footwall collapse, generating  
588 sequentially rotating crescent-shaped extensional fault blocks that became trapped as  
589 extensional horses in the footwall of the releasing bend (**Figure 11**). In the areas of the  
590 most pronounced extension the crestal part of the rotational fault blocks became  
591 elevated above the basin floor, generating ridges that influenced the basin floor  
592 topography and hence, the sedimentation. By continued sieving of sand layer on the top  
593 of these structures, forced folds (Hamblin 1965; Stearns 1978; Groshong 1989; Khalil  
594 & McClay 2016) were generated (**Figure 10A**). In the analysis we used the term *PSE-*  
595 *3-structures* for these features.

596 By a shear displacement of 0.55 cm additional curved splay faults were initiated from  
597 the northern tip of the master fault of fault 3f; **Figure 7**), delineating the northern  
598 margin of a rhombohedral pull-apart-basin (Mann et al. 1983; Mann 2007; Christie-  
599 Blick & Biddle 1985) and with a geometry that was indistinguishable from pull-apart  
600 basins or rhomb grabens affiliated with



601

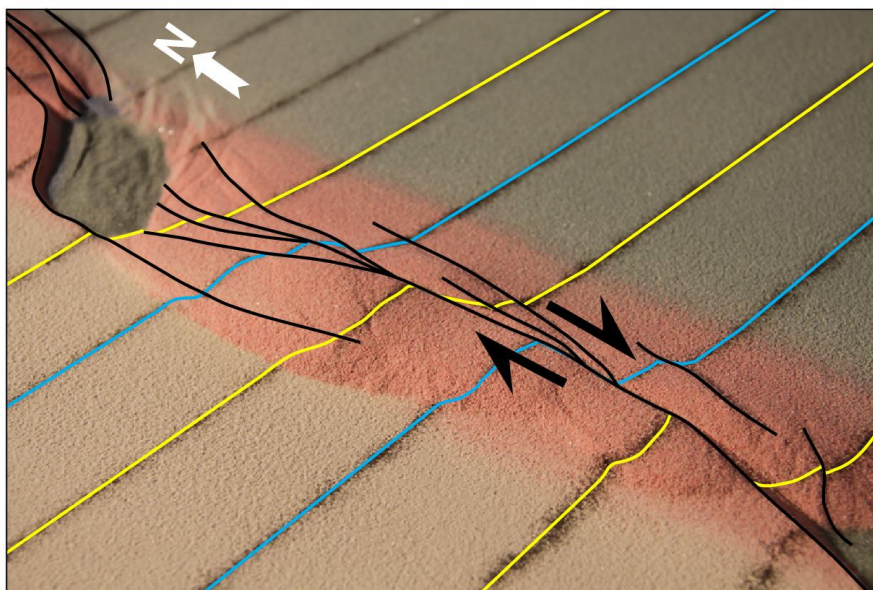
602 Figure 7: Summary of sequential activity in each master structural element (Figure 4)  
603 in Experiment BarMar6 (Figure 5). Type and amount of displacement is shown in two  
604 upper horizontal rows. The vertical blue bar indicates the stage at which full along-  
605 strike communication became established between marginal basins.  
606

607 unbridged *en échelon* fault arrays (Crowell 1974 a,b; Aydin & Nur 1993). Although  
608 sand was filled into the subsiding basins to minimize the graben relief and to prevent  
609 gravitational collapse, the sub-basins that were initiated in the shear-stage were affected  
610 by internal cross-faults, and the initial basin units remained the deepest so that the  
611 buried internal basin topography maintained a high relief with several apparent depo-  
612 centers separated by intra-basinal platforms.

613 Systems of linked shear faults and PSE's became established in the central part with  
614 neutral shear that separate the releasing and restraining bends and development  
615 similarly to that seen for segment 3 (see below), but these structures were soon  
616 destroyed by the combined development of the northern and southern tips of the  
617 extensional and contractional shear duplexes (Figure 10).

618 The first structure to develop in the regime of the restraining bend (segment 2; was a  
619 top-to-the-southwest (antithetic) thrust fault at an angle of  $145^{\circ}$  with the regional trend  
620 of the basement border as defined by segments 1 and 3 (Fault 6). It became visible by  
621 0.5 cm of displacement. The northern part of segment 2 became, however, dominated  
622 by a synthetic contractional top-to-the-northeast fault that was initiated by 0.85 cm of  
623 shear (Fault 7 Figures 5 and 6). Thus, faults 6 and 7 delineated a growing half-crescent-  
624 shaped 5-7-cm wide push-up structure (Aydin & Nur 1982; Mann et al. 1983) south of  
625 the restraining bend (Figure 9; PSE-4-structures). By continued shear these structures  
626 got the character of an antiformal stack.

627 Segment 3 defined a straight strand of neutral shear. Its development in the BarMar-  
628 experiments followed strictly that known from numerous published experiments (e.g.  
629 Tchalenko 1970; Wilcox et al. 1973; Harding 1974; Harding & Lowell 1979; Naylor et  
630 al. 1986; Sylvester 1988; Richard et al. 1991; Woodcock & Schubert 1994; Dauteuil &



631

632 Figure 8: PSE-1 anticline-syncline pairs in segment 1 experiment BarMar6 in an  
633 oblique view. PSE-1 folds were constrained to the very fault zone and the fold axes  
634 (blue lines) and extended only 3-4 cm beyond the fault zone. PSE-2 structures (incipient  
635 push-ups and positive flower structures; yellow lines) were delineated by shear faults  
636 and completely cannibalized PSE-1 structures by continued shear. Yellow and blue  
637 lines show the rotation of the fold axial trace caused by dextral shearing of c. 1,5 cm.  
638 25mm of dextral shear. By a displacement of 35mm the remains of the PSE-1 structure  
639 was completely obliterated. The distance between the markers (dark lines) is 5cm.  
640 Yellow arrow marks north-direction. White arrows indicate shear direction.

641

642 Mart 1998; Mann 2007; Casas et al. 2001; Dooley & Schreurs 2012). A train of Riedel-  
643 shears, occupying the full length of the segment, appeared simultaneously on the  
644 surface after a shear displacement of 0.5 cm, occupying a restricted zone with a width  
645 of 2-3 cm. The Riedel-shears dominated the continued structural development of  
646 Segment 3. Riedel'-shears were absent throughout the experiments, as should be  
647 expected for a sand-dominated sequence (Dooley & Schreurs 2012). P-shears  
648 developed by continued shear, creating linked rhombic structures delineated by the  
649 Riedel- and P-shears generating positive structural elements with NW-SE- and NNE-  
650 SSE-striking axes (see also Morgenstern & Tchalenko 1967), soon coalescing to form  
651 Y-shears. Transverse sections document that these structures were cored by push-up  
652 anticlines, positive half-flower structures. The segments with neutral shear would  
653 generate full-fledged positive flower structures in the advanced stages of shear (**Figures**  
654 **5 and 6**). These were accompanied by the development of *en échelon* folds and flower



655 structures as commonly reported from strike-slip faults in nature and in experiments.  
656 The width of the zone above the basal fault remained almost constant throughout the  
657 experiments, but was somewhat wider in experiments with thicker basal silicone  
658 polymer layers, similar to that commonly described from comparable experiments (e.g.  
659 Richard et al. 1991).

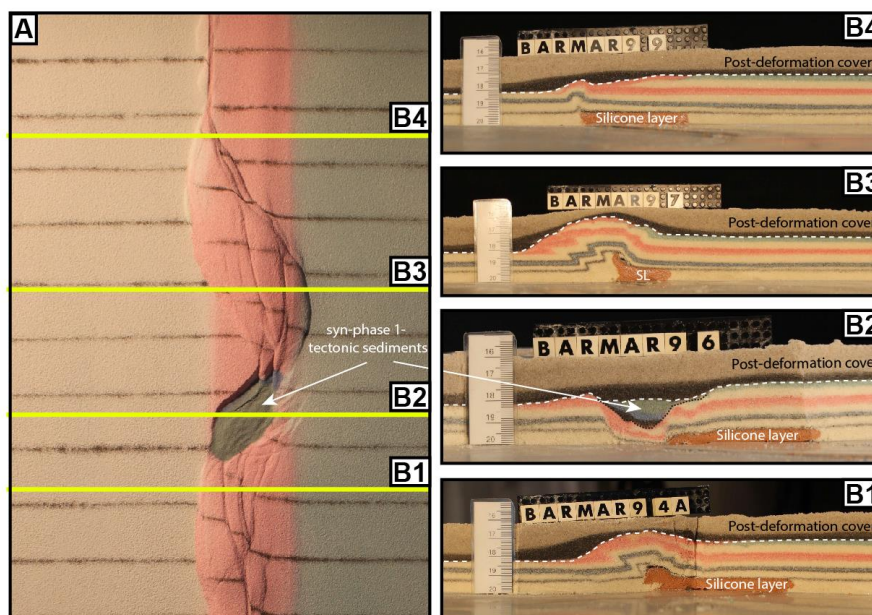
660

### 661 **Deformation Phase 2: Extension**

662 The late Cretaceous-Palaeocene dextral shear was followed by pure extension  
663 accompanying the opening along the Barents Shear Margin in the Oligocene. Our  
664 experiments utilized focused on the effects of oblique extension, acknowledging that  
665 plate tectonic reconstructions of the North Atlantic suggest an extension angle of  $325^\circ$   
666 as the most likely (Gaina et al. 2009).

667 All strike-slip basins widened in the extensional stage, and most extensively so for the  
668 experiments with orthogonal extension. The widening of the basin enhanced the  
669 topography already generated in the shear-stage in the extensional strike-slip duplex in  
670 segment 2 (PSE-3-structures). In the earliest extensional stage the strike-slip basin in  
671 segment 2 dominated the basin configuration, but by continued extension the linear  
672 segments and the minor pull-apart basins in segments 1 and 2 started to open and  
673 became interlinked, subsequently generating a linked basin system that paralleled the  
674 entire shear margin (**Figures 5F-G, 6F-G**).

675



676

677 Figure 9: Cross-sections through PSE-2-related structures. A) Folded core of incipient  
678 push-up/positive flower structure in segment 1, experiment BarMar6. The fold structure  
679 is completely enveloped of shear faults that have a twisted along-strike geometry. Note  
680 that the eastern margin of the structure developed into a negative structure at a late stage  
681 in the development (filled by black-pink sand sequence) and that the silicone putty  
682 sequence (basal pink sequence) was entirely isolated in the footwall. B) Similar  
683 structure in experiment BarMar8. The weak silicone putty layer here bridged the high-  
684 strain zone and focused folding that propagated into the sand layers (blue). The folds  
685 in upper (pink layers) were associated with the contractional stage, because they  
686 contributed to a surface relief filled in by red-black-sand sequence that was sieved into  
687 the margin during the contractional stage. C) Contraction associated with “crocodile  
688 structure” in the footwall of the main fault in segment 1, experiment BarMar8. Note  
689 disharmonic folding with contrasting fold geometries in hanging wall and footwall and  
690 at different stratigraphic levels in the footwall, indicating shifting stress situation in  
691 time and space in the experiment. D) Transitional fault strand between to more strongly  
692 sheared fault segments (experiment BarMar9).  
693

694 The orthogonal extension-phase following dextral strike-slip reactivated and very  
695 quickly linked several of the master faults that were established in deformation phase  
696 1 (Figures 5A and 6A) already by an extension of 0,25 – 0,50 cm. This included the  
697 southern fault margin, the push-up and the splay faults defining a crestal collapse  
698 graben of the push-up (Faults 6, 11 and 12; Figure 4). All three segments were  
699 reactivated in extension by c. 1.25 cm of orthogonal stretching (Figure 7). During the  
700 first cm of extension each basin remained an isolated unit, but after 1 cm of extension



701 all basins became linked, thus forming one unified elongate extensional basin (marked  
702 by the vertical dark blue line in **Figure 7**) and mainly following the PDZ as it was cut  
703 in the basal templates. Among the faults that were inactive and remained so throughout  
704 the extension phase were the antithetic contractional fault delineating the push-ups in  
705 segment 2 towards the south (Fault 6; **Figure 4**). The Y-shear in Segment 3 was  
706 reactivated as a straight, continuous extensional fault in Stage 2. Total extension in  
707 Phase 3 was 5 cm.

708

### 709 **Deformation Phase 3: contraction**

710 In our experiments the extension stage was followed by orthogonal or oblique  
711 contraction (parallel to the direction of extension as applied for each experiment). The  
712 experiments were terminated before the full closure of the basin system, i.e. the  
713 extension vector > contraction vector. A part of the early-stage contraction was  
714 accommodated along new faults. It was more common, however, that faults that had  
715 been generated in the strike-slip and extensional stages became reactivated and rotated.  
716 This was particularly the case for the master faults., as seen by continued or accelerated  
717 subsidence. The dominant structures affiliated with the contractional stage was still new  
718 folds with traces oriented orthogonal to the shortening direction and sub-parallel to the  
719 preexisting master fault systems that defined the margin and basin margins (**Figure 12**).  
720 Also some deep fold sets that had been generated during the strike-slip phase and seen  
721 as domal surface features became reactivated, causing renewed growth of surface  
722 structures (see **Figure 10** and explanation in figure caption). These folds were generally  
723 up-right cylindrical buckle folds in the initial contractional and with very large trace  
724 length: amplitude-ratio (*SPE-5-structures*). Some intra-basinal folds, however, defined  
725 fold arrays that diagonally crossed the basins. Particularly the folds situated along the  
726 basin margins developed into fault propagation-folds above low-angle thrust planes.  
727 Such faults aligning the western basin margins could have an antithetic attitude relative  
728 to the direction of contraction.

729 During the contractional phase the margin-parallel, linked basin system started  
730 immediately to narrow and several fault strands became inverted. The basin-closure  
731 was a continuous process until the end of the experiment by 3 cm of contraction. The  
732 contraction was initiated as a proxy for an ESE-directed ridge-push stage. The first  
733 effect of this deformation stage was heralded by uplift of the margin of the established



734 shear zone that that had developed into a rift during deformation stage 2. This was  
735 followed by the reactivation and inversion of some master faults (e.g. fault a2; e.g.  
736 **Figure 4**) and thereafter by the development of a new set of low-angle top-to-the-ESE  
737 contractional faults. These faults displayed a sequential development, (fault family 1;  
738 **Figure 4**) and were associated with folding of the strata in the rift structure, probably  
739 reflecting foreland-directed in-sequence thrusting.

740

741

## 742 **Discussion**

743 The break-up and subsequent opening of the Norwegian-Greenland Sea was a multi-  
744 stage event (**Figure 13**) that imposed shifting stress relation on the already  
745 geometrically complex Barents Shear Margin. The incipient stages occurred in the late  
746 Cretaceous – early Palaeocene (e.g. Eldholm et al 1987; Vågnes 1997; Myhre &  
747 Eldholm 1988; Gabrielsen et al. 1990; Gudlaugsson & Faleide. 1994; Knutsen & Larsen  
748 1997; Ryseth et al. 2003; Faleide et al. 1993; 2008; Reemst et al. 1994; Bergh & Grogan  
749 2003; Kristensen et al. 2017), and the development included extensive volcanism  
750 (Eldholm et al. 1989; Saunders et al. 1997; Planke et al. 1999; Ganerød et al. 2010;  
751 Horni et al. 2017). Opening accelerated and was accompanied by extensive marine  
752 sedimentation in the Eocene and changed into a passive margin setting from the earliest  
753 Oligocene. The spreading stage was likely associated with ridge-push (e.g. Doré &  
754 Lundin 1996; Vågnes et al. 1998; Pascal & Gabrielsen 2001), plate reorganization  
755 (Talwani & Eldholm 1977, Gaina et al. 2009) or other far-field stresses (Doré & Lundin  
756 1996; Lundin & Doré 1997; Doré et al. 1999; Lundin et al. 2013). Faults, and fold  
757 arrays associated with shear and tectonic inversion as well as elements of  
758 subsidence/elevation are obviously prominent for the deduction of the structural history  
759 in such systems (e.g. Cloos 1928, 1955; Riedel 1929; Campbell 1953; Tchalenko 1970;  
760 Wilcox et al. 1973; Dauteuil & Mart 1998; Odonne & Vialon 1983; Richard et al. 1991;  
761 Richard & Kranz 1991; Dooley & McClay 1997; Basile & Brun 1999; Mitra & Paul  
762 2011; Dooley & Schreurs 2012; Kristensen et al. 2017). Therefore, scaled experiments  
763 were designed to illuminate these complexities of the Barents Shear Margin. The  
764 experiments utilized three main segments that correspond to the Senja Fracture Zone  
765 (segment 1), the Vestbakken Volcanic Province (segment 2) and the Hornsund Fault



766 Zone (segment 3). A series of structural families developed during the experiments,  
767 most of which correspond to structural elements found along the Barents Shear Margin.  
768 Segment 1 in the experiments (which corresponds to the Senja Fracture Zone) was  
769 dominated by neutral dextral shear, although subordinate jogs in the (pre-cut) fault  
770 provided minor sub-segments with mainly releasing and subordinate restraining bends.  
771 PSE-1-folds, that developed at an incipient stage were immediately paralleled by two  
772 sets of normal faults with opposite throw in the releasing bend areas (e.g. fault 2 **Figure**  
773 **4**) so that the two faults constrained a crescent- or spindle-shaped incipient extensional  
774 shear duplex became evident (**Figures 5B and 6B**; see also Mann et al. 1983; Christie-  
775 Blick & Biddle 1985; Mann 2007; Dooley & Schreurs 2012). The most prominent of  
776 these structures corresponds to the position of the Sørvestsnaget Basin (**Figure 1B**).  
777 Structures generated at an early stage in a developing, multistage systems that involve  
778 shear, extension and contraction soon became overprinted and cannibalized by younger  
779 structures with axes parallel to the main shear fault (Y-shears). The strike-slip stage of  
780 the experiments is comparable to the experiments in series “e” and “f” of Mitra & Paul  
781 (2011). It is particularly emphasized that SPE-1 and SPE-2-structures were confined  
782 to the area just above the basal master fault (VD) and its immediate vicinity. Although  
783 careful search for positive early (PSE-1) in the reflection seismic data was conducted,  
784 no remains of such structures were detected.

785 During the oblique extension stage segment 1 of experiments BarMar7-9 were  
786 characterized by oblique opening. The basin subsidence was focused in the minor pull-  
787 apart basins, which soon became linked along the regional N-S-striking basin axis.  
788 Remains of several such basin centers, of which the Sørvestsnaget Basin (Knutsen &  
789 Larsen 1997; Kristiansen et al. 2017) is the largest, are preserved and found in seismic  
790 data (**Figure 1b**). During the experiments a continuous basin system was developed in  
791 the hangingwall side of the master fault, but it is not likely that such a superior basin  
792 system ever existed along the Barents Shear Margin.

793 In the subsequent inversion stage, fold trains with axial traces parallel (PSE-5-folds) to  
794 the basin axis and the master faults characterized segment 1. Remnants of such folds  
795 are locally preserved in the thickest sedimentary sequences affiliated with the Senja  
796 Shear Margin.

797

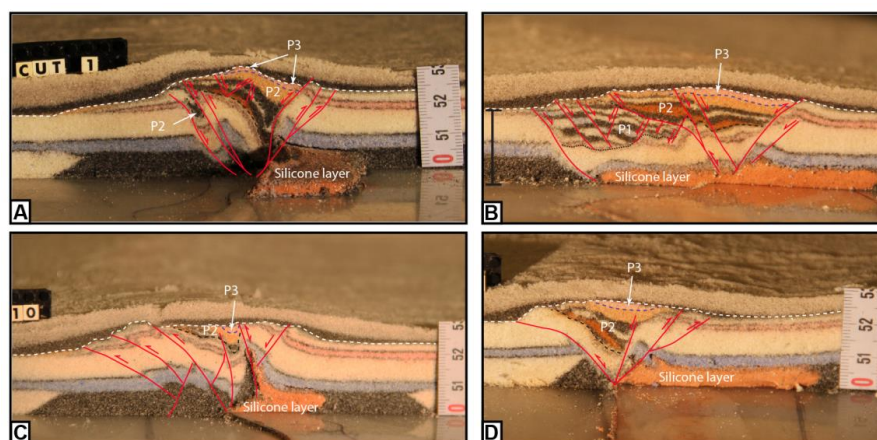
798 Segment 2, which was underlain by a crescent-shaped discontinuity corresponds to  
799 the Vestbakken Volcanic Province and the southern extension of the Knølegga Fault



800 Complex that is a branch of the southern part of the Hornsund Fault Zone (**Figure 1b**).  
801 The part of the Vestbakken Volcanic Province that was the subject of structural analysis  
802 by Giennenas (2018) corresponds to the southern part of segment 2 in the present  
803 experiments. It is dominated by interfering NNW-SSE- and NE-SW striking fold- and  
804 fault systems in the central part of the basin, whereas N-S-structures are more common  
805 along its eastern margin (**Figure 12A**) (Jebsen & Faleide 1998; Giennenas 2018).  
806 Intra-basinal platforms and complex internal configurations seen in the BarMar-  
807 experiments are common in strike-slip basins (e.g. Dooley & McClay 1997; Dooley &  
808 Schreurs 2012) and are consistent with the structural configuration with intra-basinal  
809 depo-centers within the Vestbakken Volcanic province and also in the Sørvestsnaget  
810 Basin (Knutsen & Larsen 1997; Jebsen & Faleide 1998; **Figure 13**).  
811 The positive structural elements that prevail in *segment 3* are similar to PSE-1 and PSE-  
812 2-structures described for segment 1. The structures affiliated with segment 3 in the  
813 BarMar-experiments correspond well to that seen in the reflection seismic sections  
814 along parts of the Spitsbergen and the Senja shear margins (Myhre et al. 1982). Thus,  
815 the structuring in the segment 3 in the BarMar-experiments followed strictly the pattern  
816 well established for neutral shear in that an array of NW-SE-striking *en echelon* wrench  
817 folds (termed PSE-1-structures in the description above; see Cloos 1928; Riedel 1929;  
818 Tchalenko 1970; Wilcox et al. 1973) first became visible and the development of  
819 Riedel- and P-shears. (R'-shears were subdued as expected for sand-dominated  
820 sequences (Dooley & Schreurs 2012). Continued shear followed by collapse and  
821 interaction between Riedel and P-shears and the subsequent development of Y-shears  
822 initiated push-up- and flower-structure with N-S-axes (PSE-2) structures that were  
823 expressed as non-cylindrical (double-plunging) anticlines on the surface (e.g.  
824 Tchalenko 1970; Naylor et al. 1986). Structures similar to the PSE-2-structures that  
825 were initiated in the present experiments have previously been reported from similar  
826 experiments with viscous basal layers covered by sand (e.g. Richard et al. 1991;  
827 Dauteuil & Mart 1998), and may have contributed to the more complex fold systems  
828 along the Knølegga Fault Complex.  
829 The Knølegga Fault Complex occupies a km-wide zone. The master fault strand is  
830 paralleled by faults with significant normal throws on its hanging wall side and these  
831 are considered to be strands belonging to the larger Knølegga Fault Complex (EBF;  
832 Eastern Boundary Fault; Giennenas 2018; **Figure 12A**). The EBF zone is a top-west  
833 normal fault with maximum throw of nearly 2000 m (3000 meters). It can be followed



834 along its strike for more than 60 km and seems to die out by horse-tailing at its tip-  
835 points. The vicinity of the master faults of the Knølegga Fault Complex locally display  
836 isolated elongate positive structures constrained by steeply dipping faults. These  
837 structures sometimes display internal reflection patterns that seem exotic or suspect in  
838 comparison to the surrounding sequences. Some of these structures resemble positive  
839 flower structures or push-ups or define narrow anticlines. They are found in both the  
840 footwall and hanging wall of the border faults and strike parallel to those and the axes  
841 of these structures parallel the master faults. The traces of such structures can be  
842 followed over shorter distances than the master faults, and do not occur in the central  
843 parts of the Vestbakken Volcanic Province. We speculate that these are rare fragments  
844 of dismembered EPS-2-type structures.  
845 Due to the right-stepping geometry during dextral shear in segment 2, the southern and  
846 northern parts were in the releasing and restraining bend positions,

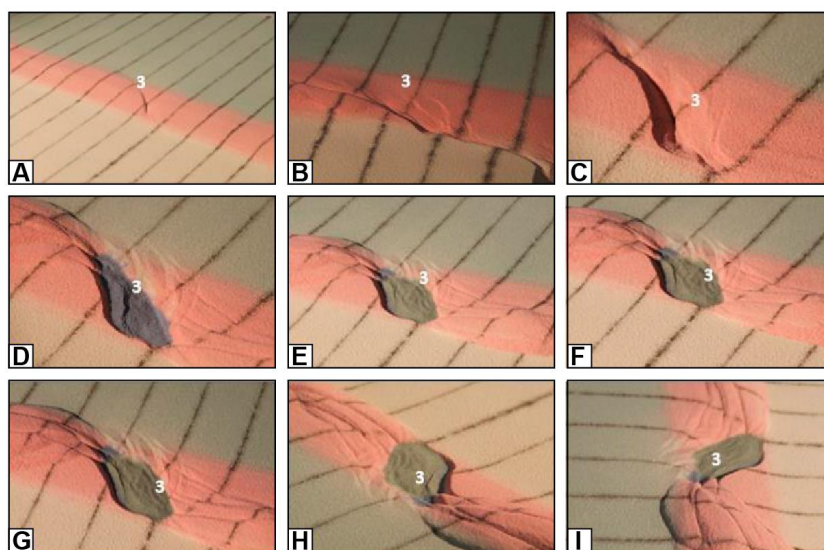


847  
848 Figure 10: A) contrasting structural styles along the master fault system in segment 2  
849 in map view and (B) cross sections of experiment BarMar9. SL denotes silicone layer,  
850 the stippled line the boundary between pre- and syn-deformation layers and the white  
851 dashed line the boundary with the post-deformation layers.  
852

853 respectively (e.g. Christie-Blick & Biddle 1985). Hence, the southern part of segment  
854 2 was subject to oblique extension, subsidence and basin formation when the northern  
855 part was subject to oblique contraction, shortening and uplift. The southern segment  
856 expanded to the east and northeast by footwall collapse and activation of rotating fault  
857 blocks that contributed to a basin floor topography that affected the pattern of sediment  
858 accumulation (**Figure 9A, B**). The crests of the rotating fault blocks are termed PSE-3-



859 structures above, and such eroded fault block crests are defining the footwalls of major  
860 faults in the Vestbakken Volcanic Province, providing space for sediment accumulation  
861 in the footwalls. The area that was affected by the basin formation in the extensional  
862 shear duplex stage seems to have remained the deepest part of the Vestbakken Volcanic  
863 Province, whereas the part formed in basin widening by sequential footwall collapse  
864 created a shallower sub-platform (*sensu* Gabrielsen 1986) (**Figure 11**). It is expected  
865 that (regional) basin and (local) fault block subsidence became accelerated during phase  
866 2 (extension), and more so in the orthogonal extension experiments (BarMar 6) than in  
867 the experiments with oblique extension (BarMar 8), but due to stabilization of basins  
868 by infilling of sand, this was not documented. The widening occurred mainly by fault-  
869 controlled collapse of the footwalls, and dominantly along the master faults that  
870 corresponded to the Knølegga Fault Complex, but also new intra-basinal cross-faults  
871 that were initiated in the shear stage (see above) became reactivated, contributing to the  
872 complexity of the basin topography.



873  
874 Figure 11: Nine stages in the development of the extensional shear duplex system above  
875 the releasing bend in experiment BarMar9. The master faults that developed at an  
876 incipient stage (e. Fault 3 that constrained the eastern margin of the extensional shear  
877 duplex) remained stable and continued to be active throughout the experiment (Figure  
878 7), but became overstepped by faults in its footwall that became the basin contraction  
879 faults at the later stages H and I. Note that the developing basement was stabilized by  
880 infilling of gray sand during this part of the experiment. Note that Fault 3 remained  
881 active and broke through the basin infill also after the basin infill overstepped the  
882 original basin margin. The distance between the markers (dark lines) is 5cm. Yellow  
883 arrow marks north-direction.

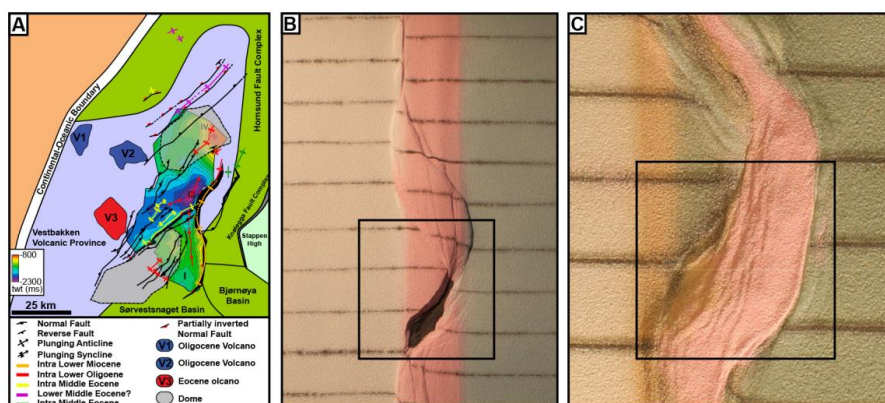


884 Referring the reflection seismic data from the Barents Shear Margin, it is not likely that  
885 a stage was reached where all basins along the margin became fully linked, although  
886 sedimentary communication along the margin is likely.

887 The contraction (phase 3) clearly reactivated normal faults, probably causing focusing  
888 of hanging wall strain and folding, rotation of fault blocks and steepening of faults. This  
889 means that both intra-basinal and marginal faults in the Vestbakken Volcanic Province  
890 can have suffered late steepening. Contraction expressed as fold systems with fold axes  
891 paralleling the basin margins development seems to correspond very well to the  
892 observed structural configuration of the Vestbakken Volcanic Province. Here  
893 pronounced tectonic inversion is focused along the N-S-striking basin margins and  
894 along some NE-SW-striking faults in the central parts of the basin. Pronounced  
895 shortening also occurred inside individual reactivated fault blocks either by bulging of  
896 the entire sedimentary sequence or as trains of folds (**Figure 12**).

897

898 The restraining bend configuration in the northern part of segment 2 was characterized  
899 by increasing contraction across strike-slip fault strands that splayed out to the  
900 northwest from the central part of segment 2 in an early stage of dextral shear.. This  
901 deformation was terminated by the end of phase 1 by



902

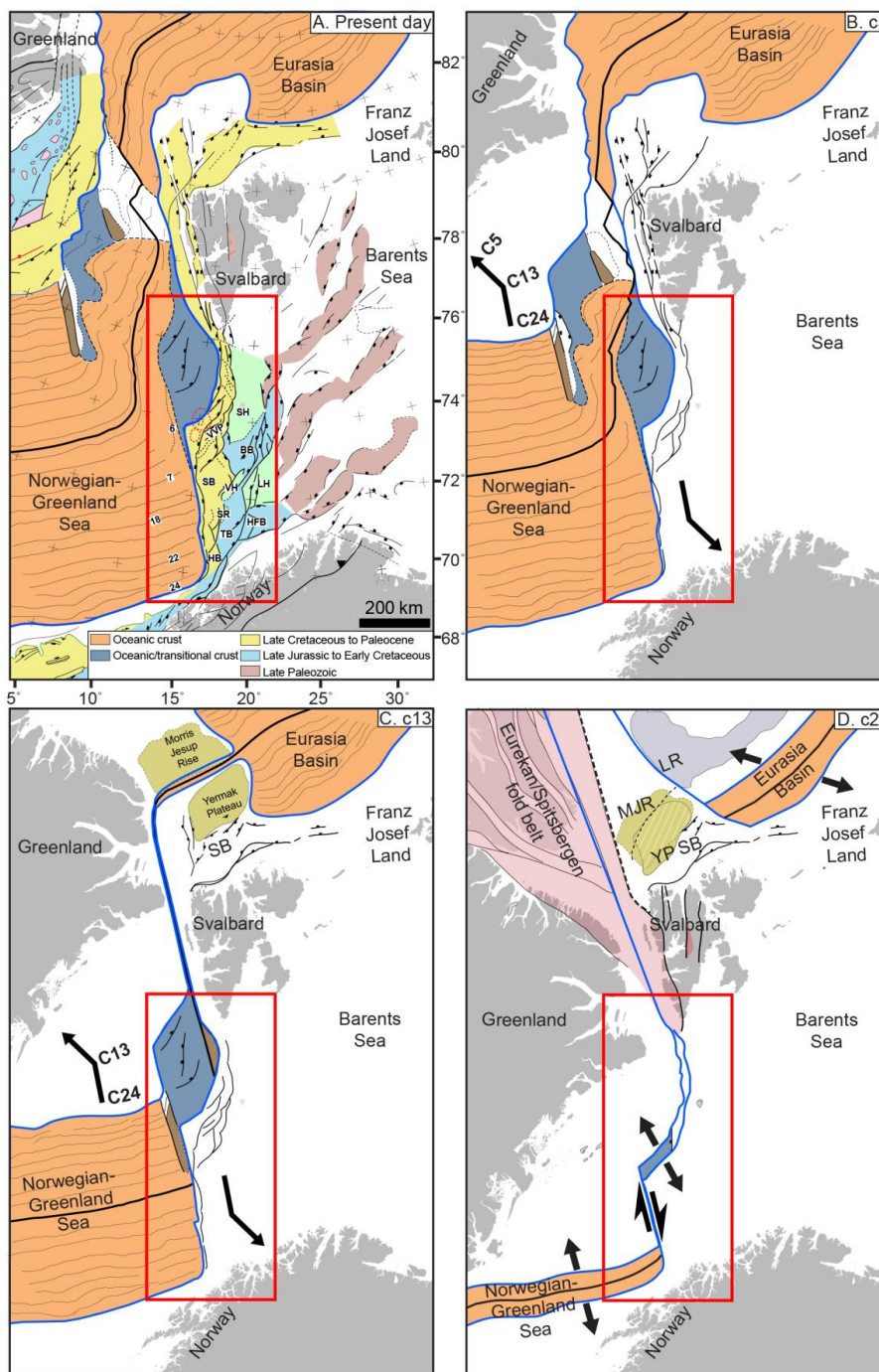
903 Figure 12: PSE-5-folds generated during phase 3-inversion, experiment BarMar8. Note  
904 that fold axes mainly parallel the basin rims, but that they deviate from that in the central  
905 parts of the basins in some cases. Note that the folds are best developed in segment 2,  
906 which accumulated extension in the combined shear and extension stages.

907

908 stacking of oblique contraction faults (PSE-4-structures), defining an antiformal  
909 stack-like structure. This type of deformation falls outside the main area, but to the



910 north this type of oblique shortening during the Eocene (phase 1) was accommodated  
911 by regional-scale strain partitioning (Leever et al. 2011a,b).  
912 The Vestbakken Volcanic Province is characterized by extensive regional shortening.  
913 Onset of this event of inversion/contraction is dated to early Miocene (Jebsen & Faleide  
914 1998, Giennenas 2018) and this deformation included two main structural fold styles.  
915 The first includes upright to steeply inclined closed to open anticlines that are typically  
916 present in the hanging wall of master faults. These folds typically have wavelengths in  
917 the order of 2.5 to 4.5 kilometers, and amplitudes of several hundred meters. Most  
918 commonly they appear with head-on snakehead-structures and are interpreted as buckle  
919 folds, albeit a component shear may occur in the areas of the most intense deformation,  
920 giving a snake-head-type geometry. The second style includes gentle to open anticline-  
921 syncline pairs with upright or steep to inclined axial planes open anticlines-synclines  
922 with wavelengths in the order of 5 to 7 kilometers and amplitudes of several tens of  
923 meters to several hundred meters. We associate those with the PSE-4-type structures as  
924 defined in the BarMar-experiments, where folds of the former type are situated in  
925 positions here sedimentary sequences have been pushed against buttresses provided by  
926 master faults along the basin margins, whereas the latter type was developed as fold  
927 trains in the interior basins, where buttressing against larger fault walls was uncommon.  
928 Also this pattern fits well with the development and geometry seen in the BarMar-  
929 experiments, where folding started in the central parts of the closing basins before  
930 folding of the marginal parts of the basin. In the closing stage the folding and inversion  
931 of master faults remained focused along the basin margins.  
932 The experiments clearly demonstrated that contraction by buckle folding was the main  
933 shortening mechanism of the margin-parallel basin system generated in phase 2  
934 (orthogonal or oblique extension) in all segments. In the Vestbakken Volcanic Province  
935 segments of the Knølegga Fault Complex, the EBF and the major intra-basinal faults  
936 contain clear evidence for tectonic inversion, whereas this is less pronounced in others.  
937 The hanging wall of the EBF is partly affected by fish-hook-type inversion anticlines  
938 (Ramsey & Huber 1987; Griera et al. 2018) (**Figure 2D, E**), or isolated hanging wall  
939 anticlines or pairs or trains of synclines and anticlines (e.g.; Roberts 1989; Coward et  
940 al. 1991; Cartwright 1989; Mitra 1993; Uliana et al. 1995; Beauchamp et al. 1996;  
941 Gabrielsen et al. 1997; Henk & Nemcok 2008), the fold style and associated faults  
942 probably being influenced by the orientation and steepness of the pre-inversion fault  
943 (Williams et al. 1989; Cooper et al. 1989; Cooper & Warren 2010).



944  
 945

Figure 13: Main stages in opening of the North Atlantic.



946 Some structures of this type can still be followed for many kilometers having consistent  
947 geometry and attitude. These structures have not been much modified by reactivation  
948 and are invariably found in the proximal parts footwalls of master faults, suggesting  
949 that these are inversion structures correlate to EPS-type 5-structures in the experiments  
950 developed in areas of focused contraction along pre-existing fault scarps during  
951 Oligocene inversion.

952 Trains of folds with smaller amplitudes and higher frequency are sometimes found in  
953 fault blocks in the central part of the Vestbakken Volcanic Province (**Figure 12F**).  
954 Although these structures are not dateable by seismic stratigraphical methods (on-lap  
955 configurations etc.) we regard these fold strains to be correlatable with the tight folds  
956 generated in the inversion stage in the experiments (EPS-5-structures) and that they are  
957 contemporaneous with the EPS-type5-structures.

958 Segment 1 in the experiments that corresponds to the Senja Shear Margin displays a  
959 structural pattern that is a blend done between configurations done in segments 1 and  
960 2, and the general conclusions drawn above are valid for this part of the shear margin.  
961

## 962 **Summary and conclusions**

963 The Barents Shear Margin is a challenging target for structural analysis both because it  
964 represents a geometrically complex structural system with a multistage history, but also  
965 because high-quality (3D) reflection seismic data are limited and many structures and  
966 sedimentary systems generated in the earlier tectonothermal stages have been  
967 overprinted and obliterated by younger events. This makes analogue experiments very  
968 useful in the analysis, since they offer a template for what kind of structural elements  
969 can be expected. By constraining the experimental model according to the outline of  
970 the margin geometry and imposing a dynamic stress model in harmony according to  
971 the state-of-the-art knowledge about the regional tectono-sedimentological  
972 development, we were able to interpret the observations done in reflection seismic data  
973 in a new light.

974

975 Our observations confirmed that the main segments of the Barents Shear Margin, albeit  
976 undergoing the same regional stress regime, display contrasting structural configurations  
977



978 The deformation in segment 2 in the BarMar-experiments, was determined by releasing  
979 and restraining bends in the southern and northern parts, respectively. Thus, the  
980 southern part, corresponding to the Vestbakken Volcanic Province, was dominated by  
981 the development of a regional-scale extensional shear duplex as defined by Woodcock  
982 & Fischer (1983) and Twiss & Moores (2007). By continued shear the basin developed  
983 into a full-fledged pull-apart basin or rhomb graben (Crowell 1974; Aydin & Nur 1982)  
984 in which rotating fault blocks were trapped. The pull-apart-basin became the nucleus  
985 for greater basin systems to develop in the following phase of extensional and also  
986 provided the space for folds to develop in the contractional phase.

987  
988 We conclude that fault- and fold systems found in the realm of the Vestbakken Volcanic  
989 Province are in accordance with a three-stage development that includes dextral shear,  
990 (oblique) extension and contraction along a shear margin with composite geometry.  
991 Folds with NE-SW-trending fold axes that are dominant in wider area of the  
992 Vestbakken Volcanic Province and are dominated by folds in the hanging walls of  
993 (older) normal faults, sometimes characterized by narrow, snake-head- or harpoon-type  
994 structures that are typical for tectonic inversion (Cooper et al. 1989; Coward 1994;  
995 Allmendinger 1998; Yameda & McClay 2004; Pace & Calamitra 2014) typical of  
996 inverted faults.

997  
998 Comparing seismic mapping and analogue experiments it is evident that a main  
999 challenge in analyzing the structural pattern in shear margins of complex geometry and  
1000 multiple reactivation is the low potential for preservation of structures that were  
1001 generated in the earliest stages of the development.

1002  
1003  
1004  
1005  
1006  
1007  
1008  
1009  
1010  
1011



1012 **Code/Data availability**

1013 The seismic data that support the findings of this study are available from NPD and  
1014 TGS. Restrictions apply to the availability of these data, which were used under license  
1015 for this study.

1016

1017 **Author contribution**

1018 R.H.Gabrielsen: Contributions to outline, design and performance of experiments. First  
1019 writing and revisions of manuscript. First drafts of figures.

1020 P.A.Giennenas: Seismic interpretation in the Vestbakken Volcanic Province.  
1021 Identification and description of fold families.

1022 D.Sokoutis: Main responsibility for set-up, performance and handling of experiments.  
1023 Revisions of manuscript.

1024 E.Willigshofer: Performance and handling of experiments. Revisions of manuscript.  
1025 Design and revisions of figure material.

1026 M.Hassaan: Background seismic interpretation. Discussions and revisions of  
1027 manuscript. Design and revisions of figure material.

1028 J.I.Faleide: Regional interpretations and design of experiments. Participation in  
1029 performance and interpretations of experiments. Revisions of manuscript, design and  
1030 revisions of figure material.

1031

1032 **Competing interests**

1033 At least one of the (co-)authors (Ernst Willingshofer) is a guest member of the editorial  
1034 board of Solid Earth for special issue (Analogue modelling of basin inversion). To the  
1035 best of our knowledge, no other conflict of interest, financial or other, exists.

1036

1037 **Acknowledgements**

1038 The study is supported by the ARCEX (Research Centre for Arctic Petroleum  
1039 Exploration) and Trias North projects which are funded by the Research Council of  
1040 Norway (grant number 228107 and 34152 respectively) together with several academic  
1041 and industry partners. We want to thank all academic institutes, industry and funding  
1042 partners. Muhammad Hassaan and Jan Inge Faleide was additionally financed by the  
1043 Suprabasins project (Research Council of Norway grant no. 295208). We also  
1044 acknowledged support staff of the Tectonic Modelling laboratory (“TecLab”) at the  
1045 Utrecht University, Netherlands for providing help to perform the analog experiments.



1046 Schlumberger is thanked for providing academic licenses to the Petrel© software. The  
1047 Norwegian Petroleum Directorate (NPD) and TGS-NOPEC Geophysical Company  
1048 ASA are also acknowledged for providing access to the regional 2D seismic data. The  
1049 technical contents and ideas presented herein are solely the authors' interpretations.  
1050  
1051



1052 **References**

- 1053
- 1054 Allemand P. & Brun J.P., 1991: Width of continental rifts and rheological layering of  
1055 the lithosphere. *Tectonophysics*, 188, 63-69.
- 1056 Allmendinger, R.W., 1998: Inverse and forward numerical modeling of threeshear fault-  
1057 propagation folds, *Tectonics*, 17(4), 640-656.
- 1058 Auzemery, A., E. Willingshofer, D. Sokoutis, J.P. Brun, S.A.P.L. Cloetingh, 2021:  
1059 Passive margin inversion controlled by stability of the mantle lithosphere,  
1060 *Tectonophysics*, 817, 229042, 1-17, <https://doi.org/10.1016/j.tecto.2021.229042>
- 1061 Aydin, A. & Nur, A., 1982: Evolution of pull-apart basins and their scale independence.  
1062 *Tectonics*, 1, 91-105.
- 1063
- 1064 Ballard J-F., Brun J-P. & Van Ven Driessche J., 1987: Propagation des chevauchements  
1065 au-dessus des zones de décollement: modèles expérimentaux. *Comptes Rendus de*  
1066 *l'Académie des Sciences, Paris*, 11, 305, 1249-1253.
- 1067
- 1068 Basile, C., (2015) Transform continental margins – Part 1: Concepts and models.  
1069 *Tectonophysics*, 661, pp.1-10. doi: 10.1016/j.tecto.2015.08.034
- 1070
- 1071 Basile, C. & Brun, J.-P., 1997: Transtensional faulting patterns ranging from pull-apart  
1072 basins to transform continental margins: an experimental investigation, *Journal of*  
1073 *Structural Geology*, 21, 23-37.
- 1074
- 1075 Beauchamp, W., Barazangi, M., Demnati, A. & El Alji, M., 1996: Intracontinental rifting  
1076 and inversion: Missouri Basin and Atlas Mountains, Morocco. *American Association of*  
1077 *Petroleum Geologists Bulletin*, 80(9), 1455-1482.
- 1078
- 1079 Bergh, S.G., Braathen, A. & Andresen, A., 1997: Interaction of basement-involved and  
1080 thin-skinned tectonism in the Tertiary fold-and-thrust belt of Central Spitsbergen,  
1081 Svalbard. *American Association of Petroleum Geologists Bulletin*, 81(4), 637-661.
- 1082
- 1083 Bergh, S.G. & Grogan, P., 2003: Tertiary structure of the Sørkapp-Hornsund Region,  
1084 South Spitsbergen, and implications for the offshore southern extension of the fold-  
1085 thrust-belt. *Norwegian Journal of Geology*, 83, 43-60.
- 1086
- 1087 Biddle, K.T. & Christie-Blick, N., (eds.), 1985a: Strike-Slip Deformation, Basin  
1088 Formation, and Sedimentation: Society of Economic Paleontologists and Mineralogists  
1089 Special Publication, 37, 386pp.
- 1090
- 1091 Biddle, K.T. & Christie-Blick, N., 1985b. Glossary — Strike-slip deformation, basin  
1092 formation, and sedimentation, in: Biddle, K.T., and Christie-Blick, N. (eds.): *Strike-*  
1093 *Slip Deformation, Basin Formation, and Sedimentation: Society of Economic*  
1094 *Paleontologists and Mineralogists Special Publication*, 37, 375-386.
- 1095
- 1096 Blaich, O.A., Tsikalas, F. & Faleide, J.I., 2017: New insights into the tectono-  
1097 stratigraphic evolution of the southern Stappen High and the transition to Bjørnøya  
1098 Basin, SW Barents Sea, *Marine and Petroleum Geology*, 85, 89-105, doi:  
1099 10.1016/j.marpetgeo.2017.04.015.



- 1100  
1101 Breivik,A.J., Faleide,J.I. & Gudlaugsson,S.T., 1998: Southwestern Barents Sea margin:  
1102 late Mesozoic sedimentary basins and crustal extension, *Tectonophysics*, 293, 21-44.  
1103  
1104 Breivik,A.J., Mjelde,R., Grogan,P., Shinamura,H., Murai,Y. & Nishimura,Y., 2003:  
1105 Crustal structure and transform margin development south of Svalbard based on ocean  
1106 bottom seismometer data. *Tectonophysics*, 369, 37-70.
- 1107 Brekke, H., 2000, The tectonic evolution of the Norwegian Sea continen- tal margin  
1108 with emphasis on the Vøring and Møre basins: Geological Society, London, Special  
1109 Publication, 136, 327–378.
- 1110 Brekke, H. & Riis, F., 1987: Mesozoic tectonics and basin evolution of the Norwegian  
1111 Shelf between 60°N and 72°N. *Norsk Geologisk Tidsskrift*, 67, 295-322.  
1112  
1113 Burchfiel,B.C. & Stewart,J.H.,1966: "Pull-apart" origin of the central segment of Death  
1114 Valley, California. *Geological Society of America Bulletin.*, 77, 439-442.  
1115  
1116 Campbell,J.D., 1958: *En échelon* folding, *Economical Geology*, 53(4), 448-472.  
1117  
1118 Cartwright,J.A.,1989: The kinematics of inversion in the Danish Central Graben. in:  
1119 M.A.Cooper & G.D.Williams (eds.): *Inversion Tectonics*. Geological Society of  
1120 London Special Publication, 44, 153-175.  
1121  
1122 Casas, A.M., Gapals,D., Nalpas,T., Besnard,K. & Román-Berdiel,T., 2001: Analogue  
1123 models of transpressive systems, *Jornal of Structural Geology*, 23,733-743.  
1124  
1125 Christie-Blick,N. & Biddle,K.T.,1985: Deformation and basin formation along strike-  
1126 slip faults. in: Biddle,K.T. & Christie-Blick,N. (eds.): *Strike-slip deformation, basin*  
1127 *formation and sedimentation*. Society of Economic Mineralogists and Palaeontologists  
1128 (Tulsa Oklahoma), Special Publication, 37, 1-34.  
1129  
1130 Cloos,H., 1928: Experimenten zur inneren Tectonick, *Zentralblatt für Mineralogie,*  
1131 *Geologie und Palaentologie*, 1928B, 609-621.  
1132  
1133 Cloos,H., 1955: Experimental analysis of fracture patterns, *Geological Society of*  
1134 *America Bulletin*, 66(3), 241-256.  
1135  
1136 Cooper,M. & Warren,M.J., 2010: The geometric characteristics, genesis and petroleum  
1137 significance of inversion structures, in Law,R.D., Butler,R.W.H., Holdsworth,R.E.,  
1138 Krabbendam,M. & Strachan,R.A. (eds.): *Continental Tectonics and Mountain*  
1139 *Building: The Lagacy of Peache and Horne*, Geological Society of London, Special  
1140 Publication, 335, 827-846.  
1141  
1142 Cooper,M.A., Williams,G.D., de Graciansky,P.C., Murphy,R.W., Needham,T., de  
1143 Paor,D., Stoneley,R., Todd,S.P., Turner,J.P. & Ziegler,P.A., 1989: Inversion tectonics  
1144 – a discussion. Geological Society, London, Special Publications, 44, 335-347.  
1145  
1146 Coward,M., 1994: Inversion tectonics, in: Hancock,P.L. (ed.): *Continental*  
1147 *Deformation*, Pergamon Press, 289-304.



- 1148  
1149 Coward,M.P., Gillcrist,R. & Trudgill,B., 1991: Extensional structures and their tectonic  
1150 inversion in the Western Alps, *in*: A.M.Roberts, G.Yielding & B.Freeman (eds.): The  
1151 Geometry of Normal Faults. Geological Society of London Special Publication, 56, 93-  
1152 112.  
1153  
1154 Crowell,J., 1962: Displacement along the San Andreas Fault, California, Geological  
1155 Society of America Special Papers, 71, 59pp.  
1156  
1157 Crowell,J.C.,1974a: Origin of late Cenozoic basins in southern California. in R.H.Dorr  
1158 & R.H.Shaver (eds.): Modern and ancient geosynclinal sedimentation. SEPM Special  
1159 Publication, 19, 292-303.  
1160  
1161 Crowell,J.C., 1974b: Implications of crustal stretching and shortening of coastal  
1162 Ventura Basin, in: Howell,D.G. (ed.): Aspects of the geological history of the  
1163 California continental Borderland, American Association of Petroleum Geologists,  
1164 Pacific Section,Publication 24, 365-382.  
1165  
1166 Cunningham,W.D. & Mann,P. (eds.), 2007a: Tectonics of Strike-Slip Restraining and  
1167 Releasing Bends, Geological Society London Special Publication, 290, 482pp.  
1168  
1169 Cunningham,W.D. & Mann,P.: 2007b: Tectonics of Strike-Slip Restraining and  
1170 Releasing Bends, *in*: Cunningham,W.D. & Mann,P. (eds.), 2007: Tectonics of Strike-  
1171 Slip Restraining and Releasing Bends, Geological Society London Special Publication,  
1172 290, 1-12.  
1173  
1174 Dauteuil,O. & Mart,Y., 1998: Analogue modeling of faulting pattern, ductile  
1175 deformation, and vertical motion in strike-slip fault zones, *Tectonics*, 17(2), 303-310.  
1176  
1177 Del Ventisette, C., Montanari, D., Sani, F., Bonini, M., Corti, G., 2007. Reply to  
1178 comment by J. Wickham on “Basin inversion and fault reactivation in laboratory  
1179 experiments”. *Journal of Structural Geology* 29, 1417–1418.  
1180  
1181 Dooley,T. & McClay,K., 1997: Analog modeling of pull-apart basins, American  
1182 Association of Petroleum Geologists Bulletin, 81(11), 1804-1826.  
1183  
1184 Dooley,T.P. & Schreurs,G., 2012:Analogue modelling of intraplate strike-slip  
1185 tectonics: A review and new experimental results, *Tectonophysics*, 574-575, 1-71.  
1186  
1187 Doré,A.G. & Lundin,E.R.,1996: Cenozoic compressional structures on the NE Atlantic  
1188 margin: nature, origin and potential significance for hydrocarbon exploration.  
1189 *Petroleum Geosciences*, 2, 299-311.  
1190  
1191 Doré,A.G., Lundin,E.R., Gibbons,A., Sømme,T.O. & Tørubakken,B.O., 2016:  
1192 Transform margins of the Arctic: a synthesis and re-evaluation *in*: Nemcok,M.,  
1193 Rybár,S., Sinha,S.T., Hermeston,S.A. & Ledvényiová,L. (eds.): Transform Margins,:  
1194 Development, Control and Petroleum Systems, Geological Society London, Special  
1195 Publication, 431, 63-94.  
1196



- 1197 Doré,A.G., Lundin,E.R., Jensen,L.N., Birkeland,Ø., Eliassen,P.E. & Fichler,C.,1999:  
1198 Principal tectonic events in the evolution of the northwest European Atlantic margin.  
1199 In: A.J.Fleet & S.A.R.Boldy (eds.): Petroleum Geology of Northwest Europe:  
1200 Proceedings of the Fifth Conference (Geological Society of London), 41-61.  
1201  
1202 Eidvin,T., Goll,R.M., Grogan,P., Smelror,M. & Ulleberg,K. 1998: The Pleistocene to  
1203 Middle Eocene stratigraphy and geological evolution of the western Barents Sea  
1204 continental margin ta well site 731675-1 (Bjørnøya West area). Norsk Geologisk  
1205 Tidsskrift, 78, 99-123.  
1206  
1207 Eidvin,T., Jansen,E. & Riis,F.,1993: Chronology of Tertiary fan deposits off the  
1208 western Barents Sea: Implications for the uplift and erosion history of the Barents Shelf.  
1209 Marine Geology, 112, 109-131.  
1210  
1211 Eldholm,O., Faleide,J.I. & Myhre,A.M., 1987: Continent-ocean transition at the  
1212 western Barents Sea/Svalbard continental margin. Geology, 15, 1118-1122.  
1213  
1214 Eldholm, O., Thiede, J., and Taylor, E., 1989, Evolution of the Vøring volcanic margin,  
1215 *in:* Eldholm, O., Thiede, J., and Taylor, E., (eds.): Proceedings of the Ocean Drilling  
1216 Program, Scientific Results, 104: College Station (Ocean Drilling Program), TX, 1033–  
1217 1065.  
1218  
1219 Eldholm,O., Tsikalas,F. & Faleide,J.I., 2002: Continental margin off Norway 62-  
1220 75°N:Paleogene tectono-magmatic segmentation and sedimentation. Geological  
1221 Society of London Special Publication, 197, 39-68.  
1222  
1223 Emmons,R.C., 1969: Strike-slip rupture patterns in sand models, Tectonophysics, 7,  
1224 71-87.  
1225  
1226 Faugère,E., Brun,J.-P. & Van Den Driessche,J., 1986: Bassins asymétriques en  
1227 extension pure et en détachements:Modèles expérimentaux, Bulletin Centre Recherche  
1228 Exploration et Production Elf Aquitaine, 10(2), 13-21.  
1229  
1230 Faleide,J.I., Bjørlykke,K. & Gabrielsen,R.H., 2015: Geology of the Norwegian Shelf.  
1231 *in:* Bjørlykke,K.: Petroleum Geoscience: From Sedimentary Environments to Rock  
1232 Physics 2<sup>nd</sup> Edition, Springer-Verlag, Berlin Heidelberg, Chapter 25, 603 -637.  
1233  
1234 Faleide,J.I., Myhre,A.M. & Eldholm,O., 1988: Early Tertiary volcanism at the western  
1235 Barents Sea margin. in: A.C.Morton & L.M.Parsons (eds.): Early Tertiary volcanism  
1236 and the opening of the NE Atlantic.Geological Society of London Special Publication,  
1237 39,135-146.  
1238  
1239 Faleide, J.I., Tsikalas, F., Breivik, A.J, Mjelde, R., Ritzmann, O., Engen, Ø., Wilson, J.  
1240 & Eldholm, O., 2008: Structure and evolution of the continental margin off Norway  
1241 and the Barents Sea. Episodes, 31(1), 82-91.  
1242  
1243 Faleide,J.I., Vågnes,E. & Gudlaugsson,S.T.,1993: Late Mesozoic - Cenozoic evolution  
1244 of the south-western Barents Sea in a regional rift-shear tectonic setting. Marine and  
1245 Petroleum Geology, 10, 186-214.  
1246



- 1247 Fichler,C. & Pastore,Z., 2022: Petrology and crystalline crust in the southwestern  
1248 Barents Sea inferred from geophysical data. *Norwegian Journal of Geology*, 102, 41pp,  
1249 <https://dx.doi.org/10.17850/njg102-2-2>  
1250  
1251 Freund,R., 1971: The Hope Fault, a strike-slip fault in New Zealand, *New Zealand*  
1252 *Geological Survey Bulletin*, 86, 1-49.  
1253  
1254 Gabrielsen, R.H., 1986: Structural elements in graben systems and their influence on  
1255 hydrocarbon trap types. in: A.M. Spencer (ed.): *Habitat of Hydrocarbons on the*  
1256 *Norwegian Continental Shelf*. *Norw. Petrol. Soc. (Graham & Trotman)*, 55 - 60.  
1257  
1258 Gabrielsen,R.H., Færseth,R.B., Jensen,L.N., Kalheim,J.E. & Riis,F.,1990: Structural  
1259 elements of the Norwegian Continental Shelf. Part I: The Barents Sea Region.  
1260 *Norwegian Petroleum Directorate, Bulletin*, 6, 33pp.  
1261  
1262 Gabrielsen,R.H., Grunnaleite,I. & Rasmussen,E., 1997: Cretaceous and Tertiary  
1263 inversion in the Bjørnøyrenna Fault Complex, south-western Barents Sea. *Marine and*  
1264 *Petroleum Geology*, 142, 165-178.  
1265  
1266 Gac,S., Klitzke,P., Minakov, Alexander, Faleide.J.I. & Scheck-Wenderoth,M., 2016:  
1267 Lithospheric strength and elastic thickness of the Barents Sea and Kara Sea region,  
1268 *Tectonophysics*, 691, 120-132, doi: 10.106/j.tecto.2016.04.028.  
1269  
1270 Gaina,C., Gernigon,L. & Ball.P., 2009: Palaeocene – Recent plate boundaries in the  
1271 NE Atlantic and the formation of the Jan Mayen microcontinent. *Journal of the*  
1272 *Geological Society, London*, 166(4), 601-616.
- 1273 Ganerød,M., Smethurst,M.A., Torsvik,T.H., Prestvik,T., Rouse,S., McKenna,C., van  
1274 Hinsbergen,D.:J.J. & Hendriks,W.W.H., 2010: The North Atlantic Igneous Province  
1275 reconstructed and its relation to the Plume Generation Zone: the Antrim Lava Group  
1276 revisited. *Geophysical Journal International*, 182, 183-202, doi: 10.1111/j.1365-  
1277 246X.2010.04620.x
- 1278 Giannenas, P.A., 2018: *The Structural Development of the Vestbakken Volcanic*  
1279 *Province, Western Barents Sea. Relation between Faults and Folds*, Unpubl. Master  
1280 thesis, University of Oslo 2018, 89 pp.  
1281  
1282 Graymer,R.W., Langenheim,V.E., Simpson,R.W., Jachens,R.C. & Ponce,D.A., 2007:  
1283 Relative simple through-going fault planes at large-earthquake depth may be concealed  
1284 by surface complexity of strike-slip faults, *in*: Cunningham,W.D. & Mann,P. (eds.):  
1285 *Tectonics of Strike-Slip Restraining and Releasing Bends*, *Geological Society London*  
1286 *Special Publication*, 290, 189-201.  
1287  
1288 Griera,A., Gomez.Rivas,E. & Llorens,M.-G., 2018: The influence of layer-interface  
1289 geometry of single-layer folding. *Geological Society of London Special Publication*  
1290 487, SP487:4  
1291  
1292 Grogan,P., Østvedt-Ghazi,A.-M., Larssen,G.B., Fotland,B., Nyberg,K., Dahlgren,S. &  
1293 Eidvin,T., 1999: Structural elements and petroleum geology of the Norwegian sector  
1294 of the northern Barents sea. *in*: Fleet,A.J. & Boldry,S.A.R. (eds.): *Petroleum Geology*



- 1295 of Northwest Europe: Proceedings of the 5th Conference, Geological Society of  
1296 London, 247-259.  
1297  
1298 Groshong, R.H., 1989: Half-graben structures: balanced models of extensional fault  
1299 bend folds, Geological Society of America Bulletin, 101, 96-195.  
1300  
1301 Gudlaugsson, S.T., & Faleide, J.I., 1994: The continental margin between Spitsbergen &  
1302 Bjørnøya, in: O.Eiken (ed.): Seismic Atlas of Western Svalbard, Norsk Polarinstitutt  
1303 Meddelelser, 130, 11-13.  
1304  
1305 Gudlaugsson, S.T., Faleide, J.I., Johansen, S.E. & Breivik, A.J., 1998: Late Palaeozoic  
1306 structural development of the south-western Barents Sea. Marine and Petroleum  
1307 Geology, 15, 73-102.  
1308  
1309 Hamblin, W.K., 1965: Origin of "reverse drag" on the down-thrown side of normal  
1310 faults, Geological Society of America Bulletin, 76, 1145-1164.  
1311  
1312 Hanisch, J., 1984: The Cretaceous opening of the Northeast Atlantic. Tectonophysics,  
1313 101, 1-23.  
1314  
1315 Harding, T.P., 1974: Petroleum traps associated with wrench faults. American  
1316 Association of Petroleum Geologists Bulletin, 58, 1290-1304.  
1317  
1318 Harding, T.P. & Lowell, J.D., 1979: Structural styles, their plate tectonic habitats, and  
1319 hydrocarbon traps in petroleum provinces, American Association of Petroleum  
1320 Geologists Bulletin, 63, 1016-1058.  
1321  
1322 Harland, W.B., 1965: The tectonic evolution of the Arctic-North Atlantic Region, in:  
1323 Taylor, J.H., Ruten, M.G., Hales, A.L., Shackleton, R.M., Nairn, A.E. & Harland, W.B.,  
1324 Discussion, A Symposium on Continental Drift, Philosophical Transactions of the  
1325 Royal Society of London, Series A, 258, 1088, 59-75.  
1326  
1327 Harland, W.B., 1969: Contributions of Spitsbergen to understanding of tectonic  
1328 evolution of North Atlantic Region, American Association of Petroleum Geologists,  
1329 Memoir 12, 817-851.  
1330  
1331 Harland, W.B., 1971: Tectonic transpression in Caledonian Spitsbergen, Geological  
1332 Magazine, 108, 27-42.  
1333  
1334 Henk, A. & Nemcok, M., 2008: Stress and fracture prediction in inverted half-graben  
1335 structures. Journal of Structural Geology, 30(1), 81-97.  
  
1336 Horni, J.Á., Hopper, J.R., Blischke, A., Geisler, W.H., Stewart, M., McDermott, K.,  
1337 Judge, M., Erlendsson, Ö & Árting, U.E., 2017: Regional Distribution of Volcanism  
1338 within the North Atlantic Igneous Province. The NE Atlantic Region: A Reappraisal of  
1339 Crustal Structure, Tectonostratigraphy and Magmatic Evolution. Geological Society,  
1340 London, Special Publications, 447, 105-125, <https://doi.org/10.1144/SP447.18>  
  
1341 Horsfield, W.T., 1977: An experimental approach to basement-controlled faulting.  
1342 Geologie en Mijnbouw, 56(4), 3634-370.



- 1343  
1344 Hubbert,M.K., 1937: Theory of scale models as applied to the study of geologic  
1345 structures, Bulletin Geological Society of America, 48, 1459-1520.
- 1346 Jepsen, C. & Faleide, 1998, Tertiary rifting and magmatism at the western Barents Sea  
1347 margin (Vestbakken volcanic province). III international conference on Arctic margins,  
1348 ICAM III; abstracts; plenary lectures, talks and posters, 92.
- 1349 Khalil,S.M. & McClay,K.R., 2016: 3D geometry and kinematic evolution of  
1350 extensional fault-related folds, NW Red Sea, Egypt. in: Childs,C., Holdswort,R.E.,  
1351 Jackson,C.A.L., Manzocchi,T., Walsh,J.J & Yielding,G. (eds.): The Geometry and  
1352 Growth of Normal Faults, Geological Society, London, Special Publication 439,  
1353 doi.org/10.1144/SP439.11
- 1354  
1355 Klinkmüller, M., Schreurs, G., Rosenau, M., Kemnitz, H., 2016. Properties of  
1356 granular analogue model materials: a community wide survey. Tectonophysics  
1357 684, 23–38. <http://dx.doi.org/10.1016/j.tecto.2016.01.017.feb>.
- 1358  
1359 Knutsen,S.-M. & Larsen,K.I.,1997: The late Mesozoic and Cenozoic evolution of the  
1360 Sørvestsnaget Basin: A tectonostratigraphic mirror for regional events along the  
1361 Southwestern Barents Sea Margin? Marine and Petroleum Geology, 14(1), 27-54.
- 1362  
1363 Kristensen,T.B., Rotevatn,A., Marvik,M., Henstra,G.A., Gawthorpe,R.L. & Ravnås,R.,  
1364 2017: Structural evolution of sheared basin margins: the role of strain partitioning.  
1365 Sørvestsnaget Basin, Norwegian Barents Sea, Basin Research, 2017), 1-23,  
1366 doi:10.1111/bre.12235.
- 1367  
1368 Le Calvez,J-H- & Vendeville,B.C., 2002: Experimental designs to mode along strike-  
1369 slip fault interaction. *in*: Scellart,W.P. & Passcheir,C. (eds.). Analogue Modeling of  
1370 large-scale Tectonic Processes, Journal of Virtual Explorer, 7, 7-23.
- 1371  
1372 Leever,K.A., Gabrielsen,R.H., Sokoutis,D. & Willingshofer,E., 2011a: The effect of  
1373 convergence angle on the kinematic evolution of strain partitioning in transpressional  
1374 brittle wedges: insight from analog modeling and high resolution digital image analysis.  
1375 Tectonics, 30, TC2013, 1-25, doi: 10.1029/2009TC002649
- 1376  
1377 Leever,K.A., Gabrielsen,R.H., Faleide,J.I. & Braathen,A., 2011b: A transpressional  
1378 origin for the West Spitsbergen Fold and Thrust Belt - insight from analog modeling.  
1379 Tectonics, 30, TC2014, 1- 24, doi: 10.1029/2010TC002753
- 1380  
1381 Libak,A., Mjelde,R., Keers,H., Faleide,J.I. & Murai,Y., 2012: An intergrated  
1382 geophysical study of Vestbakken Volcanic Province, western Barents Sea continental  
1383 margin, and adjacent oceanic crust, Marine Geophysical Research, 33(2), 187-207.
- 1384  
1385 Lorenzo.J.M., 1997: Sheared continental margins: an overview, Geo-Marine Letters,  
1386 17(1), 1-3.
- 1387  
1388 Lowell, J. D., 1972: Spitsbergen Tertiary orogenic belt and the Spitsbergen fracture  
1389 zone, Geol. Soc. Am. Bull., 83, 3091–3102, doi:10.1130/0016-  
7606(1972)83[3091:STOBAT]2.0.CO;2.



- 1390 Lundin,E.R. & Doré,A.G., 1997: A tectonic model for the Norwegian passive margin  
1391 with implications for the NE Atlantic.: Early Cretaceous to break-up. *Journal of the*  
1392 *Geological Society London*, 154, 545-550.  
1393
- 1394 Lundin,E.R., Doré,A.G., Rønning,K. & Kyrkjebø.R., 2013: Repeated inversion in the  
1395 Late Cretaceous-Cenozoic northern Vøring Basin, offshore Norway, *Petroleum*  
1396 *Geoscience*, 19(4), 329-341.  
1397
- 1398 Luth,S., Willingshofer,E., Sokoutis,D. & Cloetingh,S., 2010: analogue modelling of  
1399 continental collision: Influence of plate coupling on mantle lithosphere subduction,  
1400 crustal deformation and surface topography, *Tectonophysics*, 4184, 87-102, doi:  
1401 10.1016/j.tecto2009.08.043.
- 1402 Maher, H. D., Jr., S. Bergh, A. Braathen, and Y. Ohta, 1997: Svartfjella, Eidembukta,  
1403 and Daudmannsodden lineament: Tertiary orogen-parallel motion in the crystalline  
1404 hinterland of Spitsbergen's fold-thrust belt, *Tectonics*, 16(1), 88–106,  
1405 doi:10.1029/96TC02616.
- 1406 Mandl, G., de Jong, L.N.J., Maltha, A., 1977: Shear zones in granular material. *Rock*  
1407 *Mechanics*, 9, 95–144.  
1408
- 1409 Manduit,T. & Dauteuil,O., 1996: Small scale modeling of oceanic transform zones,  
1410 *Journal of Geophysical Research*, 101(B9), 20195-20209.  
1411
- 1412 Mann,P., 2007: Global catalogue, classification and tectonic origins of restraining and  
1413 releasing bends on active and ancient strike-slip fault systems. *in*: Cunningham,W.D.  
1414 & Mann,P. (eds.), 2007: *Tectonics of Strike-Slip Restraining and Releasing Bends*,  
1415 *Geological Society London Special Publication*, 290, 13-142.  
1416
- 1417 Mann,P., Hempton,M.R., Bradley,D.C. & Burke,K.,1983: Development of pull-apart  
1418 basins. *Journal of Geology*, 91(5), 529-554.  
1419
- 1420 Masce,J. & Blarez,E., 1987: Evidence for transform margin evolution from the Ivory  
1421 Coast Ghana continental margin, *Nature*, 326, 378-381.  
1422
- 1423 McClay.K.R., 1990: Extensional fault systems in sedimentary basins. A review of  
1424 analogue model studies, *Marine and Petroleum Geology*, 7, 206-233.  
1425
- 1426 Mitra,S.,1993: Geometry and kinematic evolution of inversion structures. *American*  
1427 *Association of Petroleum Geologists Bulletin*, 77, 1159-1191.  
1428
- 1429 Mitra,S. & Paul,D., 2011: Structural geology and evolution of releasing and  
1430 restraining bends: Insights from laser-scanned experimental models, *American*  
1431 *Association of Petroleum Geologists Bulletin*, 95(7), 1147-1180.  
1432
- 1433 Morgenstern,N.R. & Tchalenko,J.S., 1967: Microscopic structures in kaolin subjected  
1434 to direct shear, *Géotechnique*, 17, 309-328.  
1435
- 1436 Mosar,J., Torsvik,T.H. & the BAT Team, 2002: Opening of the Norwegian and  
1437 Greenland Seas: Plate tectonics in mid Norway since the late Permian. in: E.Eide (ed.):



- 1438 BATLAS. Mid Norwegian plate reconstruction atlas with global and Atlantic  
1439 perspectives. Geological Survey of Norway, 48-59.  
1440
- 1441 Mouslopoulou,V., Nicol,A., Little,T.A. & Walsh,J.J., 2007: Terminations of large-  
1442 strike-slip faults: an alternative model from New Zealand, in: Cunningham,W.D. &  
1443 Mann,P. (eds.): Tectonics of Strike-Slip Restraining and Releasing Bends, Geological  
1444 Society London Special Publication, 290, 387- 415.  
1445
- 1446 Mouslopoulou,V., Nicol,A., Walsh,J.J., Beetham,D. & Stagpoole,V., 2008: Quaternary  
1447 temporal stability of a regional strike-slip and rift fault interaction. *Journal of Structural*  
1448 *Geology*, 30, 451-463.  
1449
- 1450 Myhre,A.M. & Eldholm,O.,1988: The western Svalbard margin (74-80°N). *Marine and*  
1451 *Petroleum Geology*, 5, 134-156.  
1452
- 1453 Myhre,A.M., Eldholm,O. & Sundvor,E., 1982: The margin between Senja and  
1454 Spitsbergen Fracture Zones: Implications from plate tectonics. *Tectonophysics*, 89, 33-  
1455 50.  
1456
- 1457 Naylor,M.A., Mandl,G & Sijpestijn,C.H.K., 1986: Fault geometries in basement-  
1458 induced wrench faulting under different initial stress states. *Journal of Structural*  
1459 *Geology*, 8, 737-752.  
1460
- 1461 Nemcok,M., Rybár,S., Sinha,S.T., Hermeston,S.A.& Ledvényioviá.L., 2016:  
1462 Transform margins: development, controls and petroeuem systems – an introduction. *in:*  
1463 Nemcok,M., Rybár,S., Sinha,S.T., Hermeston,S.A. & Ledvényiová,L. (eds.):  
1464 Transform Margins,: Development, Control and Petroleum Systems, Geological  
1465 Society London, Special Publication, 431, 1-38.  
1466
- 1467 Odonne, F. & Vialon, P., 1983: Analogue models of folds above a wrench fault,  
1468 *Tectonophysics*, 990,31-46.  
1469
- 1470 Pace,P. & Calamita, F.,2014: Push-up inversion structures v. fault-bend reactivation  
1471 anticlines along oblique thrust ramps: examples from the Apennines fold-and-thrust-  
1472 belt, Italy, *Journal Geological Society London*, 171, 227-238.  
1473
- 1474 Pascal,C. & Gabrielsen,R.H.,2001: Numerical modelling of Cenozoic stress patterns in  
1475 the mid Norwegian Margin and the northern North Sea. *Tectonics*, 20(4), 585-599.  
1476
- 1477 Pascal,C., Roberts,D. & Gabrielsen,R.H., 2005: Quantification of neotectonic stress  
1478 orientations and magnitudes from field observations in Finnmark, northern Norway.  
1479 *Journal of Structural Geology*, 27, 859-870.  
1480
- 1481 Peacock,D.C.P., Nixon,C.W., Rotevatn,A., Sanderson,D.J. & Zuluaga,L.F., 2016:  
1482 Glossary of fault and other fracture networks, *Journal of Structural Geology*, 92, 12-29,  
1483 doi: 10.1016/j.jgs2016.09.008.  
1484
- 1485 Perez-Garcia,C., Safranova,P.A., Mienert,J., Berndt,C. & Andreassen,K., 2013:  
1486 Extensional rise and fall of a salt diapir in the Sørvestsnaget Basin, SW Barents Sea.  
1487 *Marine and Petroleum Geology*, 46, 129-134.



- 1488  
1489 Planke, S., Alvestad, E. and Eldholm, O., 1999, Seismic characteristics of  
1490 basaltic extrusive and intrusive rocks: The Leading Edge, 18(3), 342-348. [https://doi-](https://doi-org.ezproxy.uio.no/10.1190/1.1438289)  
1491 [org.ezproxy.uio.no/10.1190/1.1438289](https://doi-org.ezproxy.uio.no/10.1190/1.1438289)  
1492  
1493 Ramberg,H., 1967: Gravity, deformation and the Earth's crust, Academic Press, New  
1494 York, 214pp.  
1495  
1496 Ramberg,H., 1981: Gravity, deformation and the Earth's crust, 2nd edition. Academic  
1497 Press, New York 452pp.  
1498  
1499 Ramsay,J.G. & Huber,M.I., 1987: The techniques of modern structural geology. Vol.  
1500 2: Folds and fractures. Academic Press, London, 309-700.  
1501  
1502 Reemst,P., Cloetingh,S. & Fanavoll,S.,1994: Tectonostratigraphic modelling of  
1503 Cenozoic uplift and erosion in the south-western Barents Sea. Marine and Petroleum  
1504 Geology, 11, 478-490.  
1505  
1506 Richard,P.D., Ballard,B., Colletta,B & Cobbold,P.R., 1989: Naissance et evolution de  
1507 failles au dessus d'un décrochement de socle: Modélisation experimental et  
1508 tomographie, C. R. Acad.Sci. Paris, 308,9, 2111-2118.  
1509  
1510 Richard,P.D. & Cobbold,P.R., 1989: Structures et fleur positives et décrochements  
1511 crustaux: mdélisation analogique et interpretation mechanique, C.R.Acad.Sci.Paris,  
1512 308, 553-560.  
1513  
1514 Richard,P. & Krantz,R.W., 1991: Experiments on fault reactivation in strike-slip mode,  
1515 Tectonophysics, 188, 117-131.  
1516  
1517 Richard,P., Mocquet,B. & Cobbold,P.R., 1991: Experiments on simultaneous faulting  
1518 and folding above a basement wrench fault, Tectonophysics, 188, 133-141.  
1519  
1520 Riedel,W., 1929: Zur Mechanik geologischer Brucherscheinungen. Centralblatt für  
1521 Mineralogie, Geologie und Palentologie, 1929B, 354-368.  
1522  
1523 Riis, F., Vollset, J. & Sand, M., 1986: Tectonic development of the western margin of  
1524 the Barents Sea and adjacent areas. in: M.T.Halbouty (ed.): Future petroleum provinces  
1525 of the World. American Association of Petroleum Geologists Memoir, 40, 661-667.  
1526  
1527 Roberts,D.G., 1989: Basin inversion in and around the British Isles, in: M.A.Cooper &  
1528 G.D.Williams (eds.): Inversion Tectonics. Geological Society of London Special  
1529 Publication, 44, 131-150.  
1530  
1531 Ryseth,A., Augustson,J.H., Charnock,M., Haugrud,O., Knutsen.,S.-M-, Midbøe,P.S.,  
1532 Opsal,J.G. & Sundsbø,G., 2003: Cenozoic stratigraphy and evolution of the  
1533 Sørvestsnaget Basin, southwestern Barents Sea. Norwegian Journal of Geology, 83,  
1534 107-130.



- 1535 Saunders, A.D., Fitton, J.G., Kerr, A.C., Norry, M.J., and Kent, R.W., 1997, The North  
1536 Atlantic Igneous Province: Geophysical Monograph 100, American Geophysical  
1537 Union, pp. 45–93.
- 1538 Scheurs,G., 1990: Experiments on strike-slip faulting and block rotation, *Geology*,  
1539 *22*,567-570.  
1540
- 1541 Schreurs, G., 2003: Fault development and interaction in distributed strike-slip shear  
1542 zones: an experimental approach. *in*: Storti,F., Holdsworth,R.E. & Salvini,F. (eds):  
1543 Intraplate Strike-slip Deformation Belts, Geological Society of London Special  
1544 Publication, 210, 35-82.  
1545
- 1546 Schreurs, G., Colletta, B., 1998. Analogue modelling of faulting in zones of continental  
1547 transpression and transtension. *in*: Holdsworth, R.E., Strachan, R.A., Dewey, J.F.  
1548 (eds.), *Continental Transpressional and Transtensional Tectonics*, Geological Society  
1549 of London Special Publication, London, 135, 59–79.  
1550
- 1551 Schreurs,G. & Colletta,B., 2003: Analogue modelling of continental transpression and  
1552 transtension. *in*: Scellart,W.P. & Passchier,C. (eds.): *Analogue Modelling of Large-*  
1553 *scale Tectonic Processes*. *Journal of the Virtual Explorer*, 7, 103-114.  
1554
- 1555 Seiler,C., Fletcher,J.M., Quigley,M.C., Gleadow,A.J & Kohn,B.P., 2010: Neogene  
1556 structural evolution of the Sierra San Felipe, Baja California: evidence of proto-gulf  
1557 transtension in the Gulf Extensional Province? *Tectonophysics*, 488(1), 87-109.  
1558
- 1559 Sims,D., Ferrill,D.A., & Stamatakos,J.A., 1999: Role of a brittle décollement in the  
1560 development of pull-apart basins : experimental results and natural examples. *Journal*  
1561 *of Structural Geology*, 21, 533-554.  
1562
- 1563 Sokoutis D., 1987. Finite strain effects in experimental mullions. *Journal of Structural*  
1564 *Geology*, 9, 233-249.
- 1565 Stearns,D.W., 1978: Faulting and forced folding in the Rocky Mountains Foreland,  
1566 *Geological Society of America Memoir*, 151, 1-38.  
1567
- 1568 Sylvester,A.G. (ed); 1985: Wrench Fault Tectonics, Selected papers reprinted from the  
1569 AAPG Bulletin and other geological journals, American Association of Petroleum  
1570 Geologists Reprint Series 28,3 74pp.  
1571
- 1572 Sylvester,A.G.,1988: Strike-slip faults. *Geological Society of America Bulletin*, 100,  
1573 1666-1703.  
1574
- 1575 Talwani,M. & Eldholm,O.,1977: Evolution of the Norwegian-Greenland Sea.  
1576 *Geological Society of America Bulletin*, 88, 969-999.  
1577
- 1578 Tchalenko,J.S.,1970: Similarities between shear zones of different magnitudes.  
1579 *Geological Society of America Bulletin*, 81, 1625-1640.
- 1580 Tron, V. & Brun J-P.,1991: Experiments on oblique rifting in brittle-ductile systems.  
1581 *Tectonophysics*, 188(1/2), 71-84.



- 1582 Twiss,R.J. & Moores,E.M., 2007: Structural Geology, 2nd Edition, W.H.Freeman &  
1583 Co., New York, 736pp.  
1584
- 1585 Ueta,K., Tani,K. & Kato,T., 2000: Computerized X-ray tomography analysis of three-  
1586 dimensional fault geometries in basement-induced wrench faulting, Engineering  
1587 Geology, 56, 197-210.  
1588
- 1589 Uliana,M.A., Arteaga,M.E., Legarreta,L., Cerdan,J.J. & Peroni,G.O., 1995: Inversion  
1590 structures and hydrocarbon occurrence in Argentina. *in*: Buchanan,J.G. &  
1591 Buchanan,P.G. (eds.): Basin Inversion, Geological Society London Special  
1592 Publication, 88, 211-233.  
1593
- 1594 Vågnes,E.,1997: Uplift at thermo-mechanically coupled ocean-continent transforms:  
1595 modeled at the Senja Fracture Zone, southwestern Barents Sea. Geo-Marine Letters,  
1596 17, 100-109.
- 1597 Vågnes,E., Gabrielsen,R.H. & Haremo.P.,1998: Late Cretaceous-Cenozoic intraplate  
1598 contractional deformation at the Norwegian continental shelf: timing, magnitude and  
1599 regional implications. Tectonophysics, 300, 29-46.
- 1600 Weijermars, R., Schmeling, H., 1986. Scaling of Newtonian and non-Newtonian fluid  
1601 dynamics without inertia for quantitative modelling of rock flow due to gravity  
1602 (including the concept of rheological similarity. Physics of the Earth and Planetary  
1603 Interiors, 43, 316–330.
- 1604 Wilcox,R.E., Harding,T.P. & Selly,D.R., 1973: Basic wrench tectonics. American  
1605 Association of Petroleum Geologists Bulletin, 57, 74-69.  
1606
- 1607 Williams,G.D., Powell,C.M., & Cooper,M.A.,1989: Geometry and kinematics of  
1608 inversion tectonics. in: M.A.Cooper & G.D.Williams (eds.): Inversion Tectonics.  
1609 Geological Society of London Special Publication, 44, 3-16.  
1610
- 1611 Willingshofer,E., Sokoutis,D. & Burg,J.-P., 2005: Lithosphere-scale analogue modelling  
1612 of collision zones with a pre-existing weak zone, *in*: Gapais,D., Brun.,J.P.&  
1613 Cobbold,P.R. (eds.): DeformationMechanisms, Rhology and Tectonics: from Minerals  
1614 to the Lithosphere, Geological Society London Special Publication,43, 277-294.  
1615
- 1616 Willingshofer, E; Sokoutis, D., Beekman, Schönebeck, F., Warsitzka, J.-M., Michael,  
1617 M. & Rosenau, M., 2018: Ring shear test data of feldspar sand and quartz sand used in  
1618 the Tectonic Laboratory (TecLab) at Utrecht University for experimental Earth Science  
1619 applications. V. 1. GFZ Data Service. <https://doi.org/10.5880/figeo.2018.072>  
1620
- 1621 Woodcock,N.H. & Fisher,M.,1986: Strike-slip duplexes. Journal of Structural  
1622 Geology, 8(7), 725-735.  
1623
- 1624 Woodcock,N.H. & Schubert,C.,1994: Continental strike-slip tectonics. in:  
1625 P.L.Hancock (ed.): Continental Deformation (Pergamon Press), 251-263.  
1626
- 1627 Yamada,Y & McClay,K.R., 2004: Analog modeling of inversion thrust structures,  
1628 experiments of 3D inversion structures above listric fault systems, in: McClay,K.R.



1629 (ed.): Thrust Tectonics and Petroleum Systems, American Association of Petroleum  
1630 Geologists Memoir, 82, 276-302.  
1631